Behavioral/Cognitive

G-Protein-Gated Inwardly Rectifying Potassium (Kir3/GIRK) Channels Govern Synaptic Plasticity That Supports Hippocampal-Dependent Cognitive Functions in Male Mice

Souhail Djebari,[1*] Guillermo Iborra-Lázaro,[1*] Sara Temprano-Carazo,[1*] Irene Sánchez-Rodríguez,[1*] Mauricio O. Nava-Mesa,[1,2] Alejandro Múnera,[1,3] Agnès Gruart,[4] José M. Delgado-García,[4] Lydia Jiménez-Díaz,[1†] and Juan D. Navarro-López[1†]

[1]University of Castilla-La Mancha, NeuroPhysiology & Behavior Laboratory, Centro Regional de Investigaciones Biomédicas, Facultad de Medicina de Ciudad Real, Spain 13071, [2]Neuroscience Research Group (NEUROS), Universidad del Rosario, Bogotá, Colombia 111711, [3]Behavioral Neurophysiology Laboratory, Universidad Nacional de Colombia, Bogotá, Colombia 111321, and [4]Division of Neurosciences, Pablo de Olavide University, Seville, Spain 41013

The G-protein-gated inwardly rectifying potassium (Kir3/GIRK) channel is the effector of many G-protein-coupled receptors (GPCRs). Its dysfunction has been linked to the pathophysiology of Down syndrome, Alzheimer's and Parkinson's diseases, psychiatric disorders, epilepsy, drug addiction, or alcoholism. In the hippocampus, GIRK channels decrease excitability of the cells and contribute to resting membrane potential and inhibitory neurotransmission. Here, to elucidate the role of GIRK channels activity in the maintenance of hippocampal-dependent cognitive functions, their involvement in controlling neuronal excitability at different levels of complexity was examined in C57BL/6 male mice. For that purpose, GIRK activity in the dorsal hippocampus CA3−CA1 synapse was pharmacologically modulated by two drugs: ML297, a GIRK channel opener, and Tertiapin-Q (TQ), a GIRK channel blocker. *Ex vivo*, using dorsal hippocampal slices, we studied the effect of pharmacological GIRK modulation on synaptic plasticity processes induced in CA1 by Schaffer collateral stimulation. *In vivo*, we performed acute intracerebroventricular (i.c.v.) injections of the two GIRK modulators to study their contribution to electrophysiological properties and synaptic plasticity of dorsal hippocampal CA3−CA1 synapse, and to learning and memory capabilities during hippocampal-dependent tasks. We found that pharmacological disruption of GIRK channel activity by i.c.v. injections, causing either function gain or function loss, induced learning and memory deficits by a mechanism involving neural excitability impairments and alterations in the induction and maintenance of long-term synaptic plasticity processes. These results support the contention that an accurate control of GIRK activity must take place in the hippocampus to sustain cognitive functions.

Key words: ex vivo; hippocampus; *in vivo*; Kir3/GirK; LTP/LTD; metaplasticity

Significance Statement

Cognitive processes of learning and memory that rely on hippocampal synaptic plasticity processes are critically ruled by a finely tuned neural excitability. G-protein-gated inwardly rectifying K^+ (GIRK) channels play a key role in maintaining resting membrane potential, cell excitability and inhibitory neurotransmission. Here, we demonstrate that modulation of GIRK channels activity, causing either function gain or function loss, transforms high-frequency stimulation (HFS)-induced long-term potentiation (LTP) into long-term depression (LTD), inducing deficits in hippocampal-dependent learning and memory. Together, our data show a crucial GIRK-activity-mediated mechanism that governs synaptic plasticity direction and modulates subsequent hippocampal-dependent cognitive functions.

Received Nov. 5, 2020; revised May 11, 2021; accepted June 4, 2021.

Author contributions: S.D., G.I.-L., S.T.-C., I.S.-R., M.O.N.-M., and A.M. performed research; A.G., J.M.D.-G., L.J.-D., and J.D.N.-L. designed research; A.G., J.M.D.-G., L.J.-D., and J.D.N.-L. contributed unpublished reagents/analytic tools; S.D., G.I.-L., S.T.-C., I.S.-R., L.J.-D., and J.D.N.-L. analyzed data; A.M., L.J.-D., and J.D.N.-L. edited the paper; L.J.-D. and J.D.N.-L. wrote the first draft of the paper; L.J.-D. and J.D.N.-L. wrote the paper.

This work was supported by the Spanish Ministry of Economy and Competitiveness from MINECO-FEDER Grant BFU2017-82494-P (to L.J.-D. and J.D.N.-L.), the Fundación Tatiana Perez de Guzmán el Bueno (L.J.-D.), and the "Plan Propio de Investigación" Programmes of the University of Castilla-La Mancha (Predoctoral to I. S.-R. and G.I.-L. and Senior Visiting Researchers to M.O.N.-M. and A.M.). We thank Jose M. Gonzalez, María Sánchez, and Jose A. Santos for their excellent technical assistance and Roger Churchill for his help in the edition of the manuscript.

*S.D., G.I.-L., S.T.-C., I.S.-R. contributed equally to this work.

†L.J.-D., and J.D.N.-L. contributed equally to this work.

The authors declare no competing financial interests.

Correspondence should be addressed to Juan D. Navarro-López at juan.navarro@uclm.es or Lydia Jiménez-Díaz at lydia.jimenez@uclm.es.

https://doi.org/10.1523/JNEUROSCI.2849-20.2021

Introduction

G-protein-gated inwardly rectifying potassium (Kir3/GIRK) channels are a family of K^+ channels activated via ligand-stimulated G-protein-coupled receptors (GPCRs; González et al., 2012; Jeremic et al., 2021). The GPCR-GIRK cascade can be started by many neurotransmitters inducing neurons to hyperpolarize, contributing to resting membrane potential, cell excitability and inhibitory neurotransmission (Lüscher and Slesinger, 2010). Being the downstream physiological effectors of a variety of receptors (as shown *ex vivo* and/or *in vivo*) such as GABAergic ($GABA_B$), serotoninergic (5HT-1A), adenosinergic (A_1), muscarinic (M_2), noradrenergic ($\alpha 2$), dopaminergic (D_2, D_3, and D_4), opioid (μ, κ, and δ), cannabinoid (CB1), or somatostatin, GIRK channels have been pointed out as potential targets to be explored in many CNS disorders (for details, see Mayfield et al., 2015; Jeremic et al., 2021). GIRK-dependent signaling disruption has been related to the etiology of several disorders such as Down syndrome, epilepsy, schizophrenia, autism, mood disorders, Alzheimer's disease, and drug abuse (Nava-Mesa et al., 2014; Slesinger and Wickman, 2015; Rifkin et al., 2017; Jeremic et al., 2021).

Genetic models have afforded knowledge about the functional role of GIRK channels in normal and pathologic conditions (Mayfield et al., 2015). However, these models raise concerns about what compensatory mechanisms would occur in the case of global deletion of individual genes. In this sense, studies on the functional consequences of pharmacological modulation of GIRK channels are scarce, even after the blocker Tertiapin (Jin and Lu, 1998) and opener ML297 (Days et al., 2010) were identified years ago.

GIRK channels consist of various combinations of four homologous subunits (GIRK1–GIRK4), although there is general agreement that GIRK1/GIRK2 heteromultimers are the prototypical neural GIRK channel (Lüscher et al., 1997; Fernández-Alacid et al., 2011). GIRK channels are found in the dorsal hippocampus (Luján and Aguado, 2015), a region that predominantly executes cognitive functions (Morris, 2007; Fanselow and Dong, 2010), and their genetic manipulation interferes with memory acquisition and consolidation processes (Ostrovskaya et al., 2014; Victoria et al., 2016). GIRK channels can also be constitutively active by ambient adenosine and A_1 receptor (A_1R) activation (Chen and Johnston, 2005; Kim and Johnston, 2015), contributing to resting conductance *ex vivo* (Lüscher et al., 1997; Nava-Mesa et al., 2013) and gating long-term potentiation (LTP; Malik and Johnston, 2017), a synaptic plasticity process considered the physiological substrate for memory formation in the hippocampus (Bliss et al., 2018). They have been also proposed to participate in memory consolidation processes by modulating hippocampal sharp waves and ripples (Trompoukis et al., 2020). Therefore, GIRK channels are not only important for excitability regulation and normal synaptic transmission, but their activity might also modulate the predisposition of synapses to undergo subsequent neural plasticity processes (Sánchez-Rodríguez et al., 2017, 2020), a phenomenon known as metaplasticity (Abraham, 2008). Changes in neural excitability may modify LTP induction threshold and even generate long-term depression (LTD; Keck et al., 2017; Mayordomo-Cava et al., 2020; Sánchez-Rodríguez et al., 2020), a form of synaptic plasticity mainly associated to habituation forms of memory (Collingridge et al., 2010) and extinction of earlier memories (Malleret et al., 2010). Although GIRK activity is a pivotal determinant for hippocampal principal neurons' excitability (Drake et al., 1997; Lüscher et al., 1997; Chen and Johnston, 2005; Nava-Mesa et al., 2013; Kim and Johnston, 2015; Malik and Johnston, 2017), its contribution to cognitive processes performed by dorsal hippocampus has not been deeply investigated.

In this study, we pharmacologically modulated GIRK channel activity studying, in brain slices and behaving animals, excitability and synaptic plasticity processes in the dorsal hippocampal CA3−CA1 synapse and induction and its impact on cognition. Interestingly, GIRK modulation impaired LTP induction and maintenance and finally favored LTD generation. In addition, deficits were observed in habituation and recognition memories, as well as in operant learning. Together, our data show a key role for GIRK activity regulating synaptic plasticity direction and related hippocampal-dependent cognitive functions.

Materials and Methods

Subjects

Experiments detailed in the flowchart (Fig. 1) were conducted on 165 C57BL/6 male mice (RRID:MGI:5656552) aged 3–12 weeks old (15–32 g) obtained from an authorized distributor (Charles River). Animals were housed in groups of 5 per cage and kept on a 12/12 h light/dark (L/D) cycle with constant ambient temperature (21 ± 1°C) and humidity (50 ± 7%). Animals that underwent surgery were individually housed after such procedure. Food and water were available *ad libitum*. In all cases, animals were randomly allocated to experimental groups, and experimenters were blind to treatment.

All experiments were performed in accordance with European Union guidelines (2010/63/EU) and Spanish regulations for the use of laboratory animals in chronic experiments (RD 53/2013 on the care of experimental animals: BOE 08/02/2013) and approved by local Ethics Committees of the Universities of Castilla-La Mancha and Pablo de Olavide. All efforts were made to minimize animal suffering.

Ex vivo field EPSP (fEPSP) recordings: hippocampal slice preparation

Hippocampal slices were prepared as described previously (Sánchez-Rodríguez et al., 2020) and coronal sections were selected as Schaffer collaterals are perfectly preserved (Xiong et al., 2017; Fig. 2*A*). In brief, animals were deeply anesthetized with halothane (Fluothane, AstraZeneca), briefly intracardially perfused with 1 ml oxygenated (95% O_2 + 5% CO_2) ice-cold (4–6°C) artificial CSF (aCSF), with sucrose (234 mM; #84 100; Sigma) replacing NaCl to minimize damage, and decapitated. The brain was excised and rapidly immersed in oxygenated ice-cold aCSF containing the following: 118 mmol/l NaCl (#S9888; Sigma), 3 mmol/l KCl (#P3911; Sigma), 1.5 mmol/l $CaCl_2$ (#499609; Sigma), 1 mmol/l $MgCl_2$ (#208337; Sigma), 25 mmol/l $NaHCO_3$ (#S6014; Sigma), 30 mmol/l glucose (#G8270; Sigma), and 1 NaH_2PO_4 (#S8282; Sigma). Coronal brain slices (350 µm thick) containing the dorsal hippocampus were prepared with a vibratome (7000smz-2; Campden Instruments; Malik and Johnston, 2017). Slices were incubated, for at least 1 h, at room temperature (22°C) in oxygenated aCSF before recording.

For recording, a single hippocampal slice was transferred to an interface recording chamber (BSC-HT and BSC-BU; Harvard Apparatus) and perfused continuously with aCSF. Extracellular field potentials from the CA1 pyramidal neurons were recorded using a borosilicate glass micropipette (1−3 MΩ; RRID:SCR_008593; World Precision Instruments) filled with aCSF positioned on the slice surface in the stratum radiatum of CA1 and connected to the headstage of an extracellular recording amplifier (NeuroLog System; Digitimer). The synaptic responses were evoked by paired-pulse stimulation applied at 0.2 Hz on the Schaffer collateral pathway through a tungsten concentric bipolar stimulating electrode (World Precision Instruments) using a programmable stimulator (MASTER-9; A.M.P.I.; Fig. 2*A*). Biphasic, 60-µs-long, square-wave pulses were adjusted to ~35% of the intensity necessary for evoking a maximum fEPSP response. For the paired-pulse facilitation (PPF) protocol, stimulus intensity was set to ~35% of the intensity for evoking a maximum fEPSP response set to avoid population spikes; pairs of stimuli were then delivered at different interstimulus intervals (10, 20, 40, 100, 200, 500 ms). For input/output (I/O)

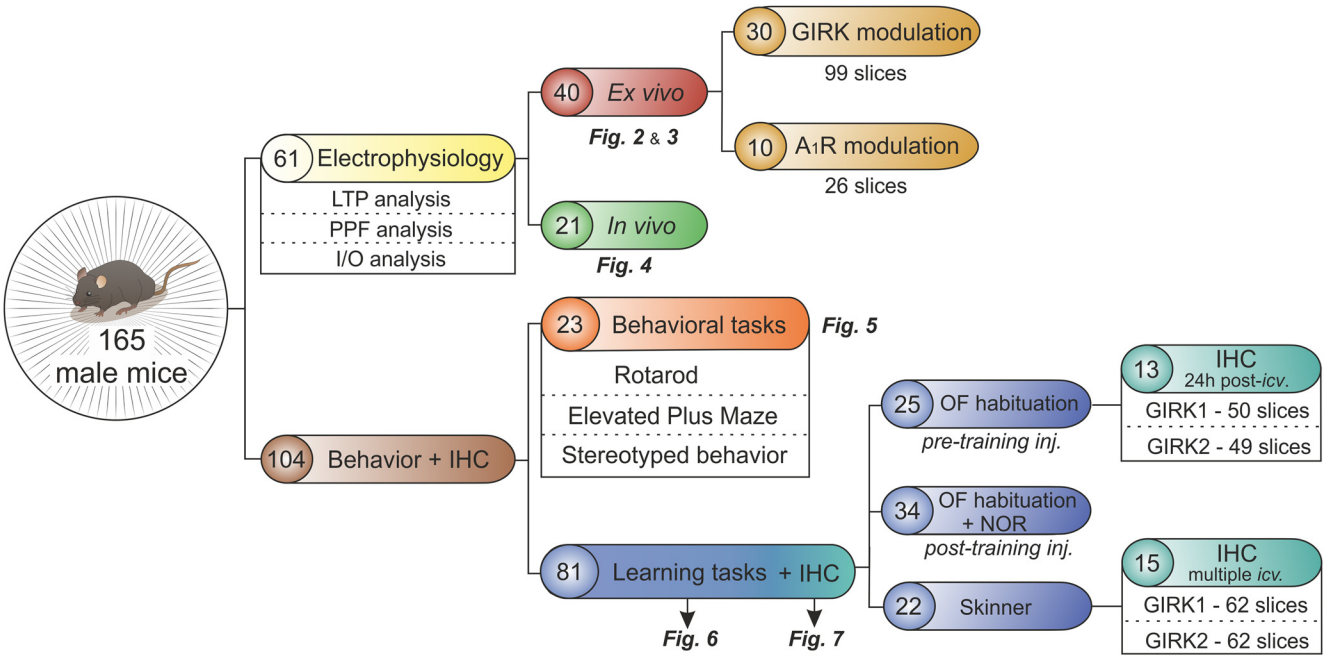

Figure 1. Distribution of animals in the experiments and corresponding figures. Circled numbers indicate the number of mice used for each specific experiment or group of experiments. Additional panels show the number of slices or, alternatively, the analyses or tasks included in a group of experiments. IHC, immunohistochemistry; OF, open field habituation test; NOR, novel object recognition test; A_1R, adenosine 1 receptor; LTP, long term potentiation; PPF, paired-pulse facilitation; I/O, input/output curves: icv., intracerebroventricular; inj., injection.

curves, two stimuli of increasing intensity (0.02–0.4 mA) were delivered at 40-ms interstimulus interval. For LTP induction (Fig. 3), a high-frequency stimulation (HFS) protocol was used, consisting of five 1-s-long 100-Hz trains delivered at 30-s intertrain interval. Baseline (BL) values of fEPSPs amplitude recorded at the CA3−CA1 synapse were collected at least 10 min before LTP induction. After LTP induction, fEPSPs were recorded during at least 60 min to evaluate early LTP (E-LTP) and late LTP (L-LTP) phases (i.e., induction and maintenance phases).

In vivo experiments: surgery

Experimental procedures used to record hippocampal fEPSPs in freely behaving mice have been described in detail elsewhere (Gruart et al., 2006; Sánchez-Rodríguez et al., 2017; Fig. 4*A*). Briefly, mice were anesthetized with 4–1.5% isoflurane (induction and maintenance, respectively; #13400264, ISOFLO, Proyma S.L.) delivered using a calibrated R580S vaporizer (RWD Life Science; flow rate: 0.5 l/min O_2). Buprenorphine was administered intramuscularly as analgesic during and after surgery (0.01 mg/kg; #062009, BUPRENODALE, Albet). Animals were implanted with bipolar stimulating electrodes aimed at the right Schaffer collateral-commissural pathway of the dorsal hippocampus (2 mm lateral and 1.5 mm posterior to bregma; depth from brain surface, 1.0–1.5 mm; Fig. 4*A*; Paxinos and Franklin, 2001), and with a recording electrode aimed at the ipsilateral stratum radiatum underneath the CA1 area (1.2 mm lateral and 2.2 mm posterior to bregma; depth from brain surface, 1.0–1.5 mm). These electrodes were made from 50-μm, Teflon-coated tungsten wire (#W558415; Advent Research Materials) and their precise location was verified histologically (Fig. 2*A*) and from fEPSP profiles.

Drugs included in this study were administered by intracerebroventricular (i.c.v.) injections that would affect the dorsal hippocampus, among other regions in the brain (DeVos and Miller, 2013; Sánchez-Rodríguez et al., 2020). For i.c.v. administration, animals were also implanted chronically with a blunted, stainless steel, 26-G guide cannula (Plastics One) aimed at the lateral ventricle (0.5 mm posterior to bregma, 1.0 mm lateral to midline, and 1.8 mm below the brain surface) in the hemisphere contralateral to the one where stimulating and recording hippocampal electrodes were placed, as described elsewhere (Sánchez-Rodríguez et al., 2017; Fig. 4*A*). Injections in freely moving mice were conducted with the help of a motorized Hamilton syringe at a rate of 0.5 μl/min through a 33-G cannula, 0.5 mm longer than the implanted guide cannula and inserted inside it, based on previous studies (Sánchez-Rodríguez et al., 2017, 2019, 2020). Temporal details of i.c.v. injections are described in each experiment.

Finally, during surgical procedure, a bare silver wire (0.1 mm in diameter) was fixed to the skull as ground (Fig. 4*A*). Stimulating and recording electrodes and the ground were connected to a 6-pin socket that was then fixed to the skull with two small anchoring screws and dental cement. Mice were allowed a week for recovery before experimental sessions. Mice were routinely handled to minimize stress during experimental procedures.

In vivo electrophysiological recordings in freely moving mice

To investigate the role of GIRK channels in hippocampal functionality *in vivo*, we studied the excitability and functional capabilities of the CA3–CA1 synapse in alert behaving mice by generating I/O curves and testing synaptic plasticity through the induction of PPF and LTP by HFS of the hippocampal Schaffer collateral pathway, as previously described (Sánchez-Rodríguez et al., 2017; Fig. 4). Only electrical recordings displaying clear field postsynaptic potential (fPSP) components, without deterioration over time, and lacking signs of epileptiform activity (stimulus-evoked after-discharges, and/or ictal or postictal activity) were selected for analysis.

The fEPSPs were obtained from alert behaving mice using Grass P511 differential amplifiers through high-impedance probes (2×10^{12} Ω, 10 pF). Schaffer collateral stimulation-evoked EPSPs were recorded from the hippocampal CA1 area, while the animal was placed in a small ($5 \times 5 \times 5$ cm) box before (BL values) and after i.c.v. injections. Electrical stimuli to Schaffer collaterals were 100-μs-long, square, biphasic pulses delivered either alone, paired, or in trains. As described for *ex vivo* experiments, for the PPF protocol stimuli with intensity enough to evoke fEPSPs with ~35% the maximum amplitude were delivered at 0- to 500-ms interstimulus intervals. For I/O curves, two stimulus intensities ranging from 0.02 to 0.4 mA were elicited at 40-ms interstimulus interval (Gruart et al., 2006; Sánchez-Rodríguez et al., 2017).

For LTP induction in behaving mice, stimuli intensity was also set at ~35% of that evoking maximum fEPSP amplitude. An additional criterion for selecting stimulus intensity for LTP induction was that a second

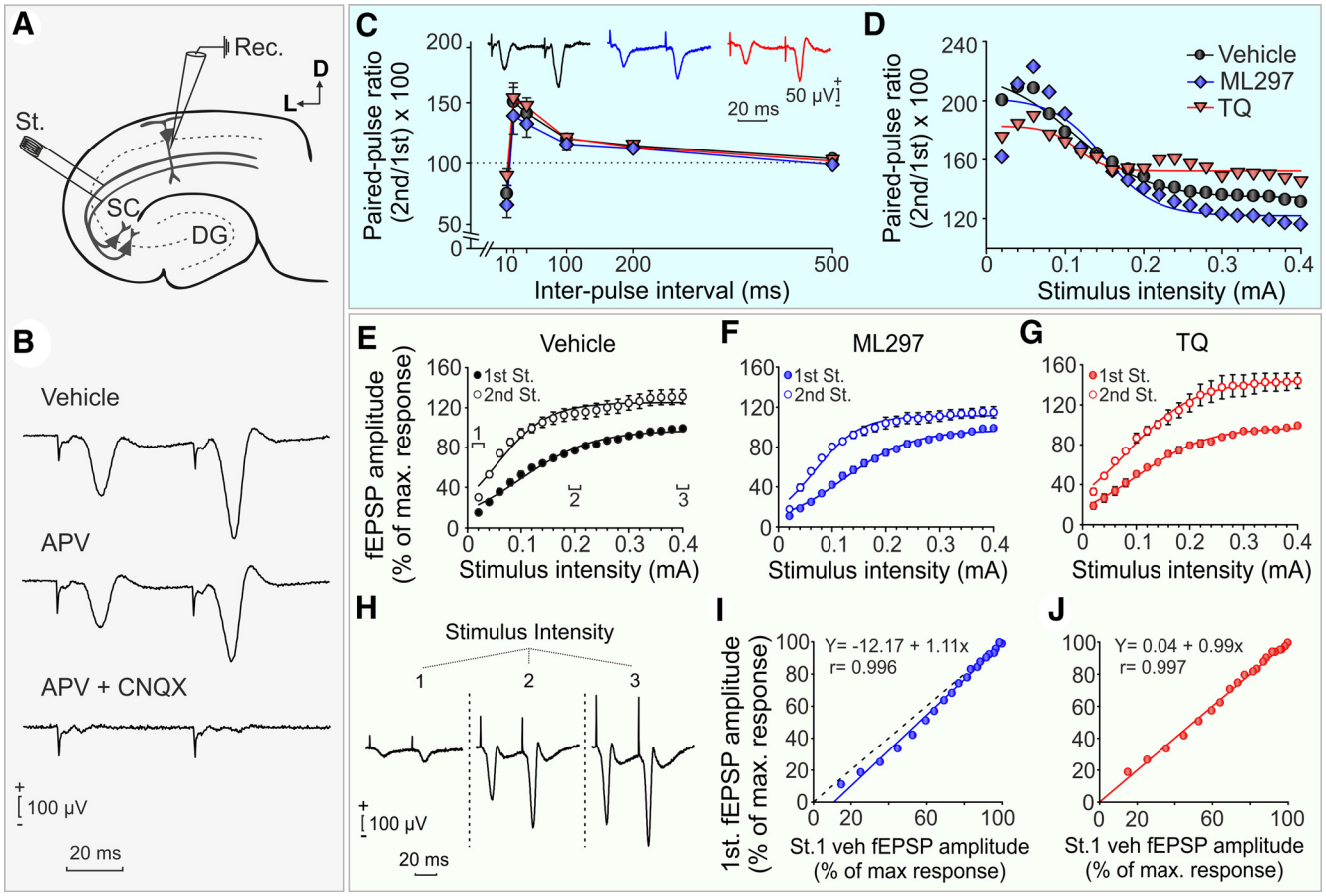

Figure 2. Role of GIRK activity on dorsal hippocampal CA3—CA1 synapse properties. ***A***, Experimental design. The diagram illustrates the location of stimulation (St.) and recording (Rec.) electrodes in a hippocampal coronal slice. SC, Schaffer collaterals; DG, dentate gyrus; L, lateral; D, dorsal. ***B***, Pharmacological characterization of the recorded fEPSPs in CA1. ***C***, PPF curve at the CA1—CA3 synapse in slices perfused with aCSF alone (vehicle), ML297 (10 μM), and TQ (0.5 μM). Averaged fEPSP paired traces for each pharmacological condition were collected at interstimulus intervals of 10–500 ms. Data are expressed as mean ± SEM amplitude of the second fEPSP expressed as a percentage of the first [(second/first) × 100] for each of the interstimulus intervals used in this test (PPR) for each experimental group. ***D***, Evolution of the PPR [(second/first) × 100] at 40-ms interstimulus interval with increasing stimulus intensity from 0.02 to 0.4 mA. ***E–G***, For the I/O curves, Schaffer collaterals were also stimulated with paired pulses at intensities to study relationship between the stimulus intensity and the amplitude of the fEPSPs evoked in CA1. fEPSP, field excitatory postsynaptic potential; max., maximum; %, percentage. ***H***, Representative recordings are shown for 0.02 (1), 0.2 (2), and 0.4 (3) mA in control slices. ***I***, ***J***, fEPSP values evoked by the paired pulses in the different experimental groups versus control (*x*-axis, vehicle; *y*-axis, experimental group). veh, vehicle. Mean ± SEM is represented in ***C***, ***E–G***.

stimulus, presented 40 ms after the first one (conditioning pulse), evoked an fEPSP with amplitude at least 150% the amplitude of the first (Bliss and Gardner-Medwin, 1973). To obtain a BL, single 100-μs-long, square, biphasic pulses delivered at 0.05 Hz to the CA3–CA1 synapse were used to elicit fEPSPs and their amplitudes were measured during 15 min before LTP. For LTP induction with HFS, six train clusters were delivered at 1 min intervals, each cluster consisted of five 100-Hz frequency, 100-ms-long pulse trains delivered at 1-s intervals; therefore, a total of 300 pulses were used in a given LTP induction session (Gruart et al., 2006; Sánchez-Rodríguez et al., 2017). To avoid inducing large population spikes and/or epileptiform activity, stimulus intensity during HFS was the same as that used during BL. Immediately after the LTP induction session, stimuli with the same parameters as for BL were delivered during 30 min. On successive days, BL stimulation parameters were used for 15-min-long recording sessions. fEPSP amplitude data during the HFS session and afterward were normalized using BL fEPSP values collected on the first day as 100%; in this manner, it was possible to monitor fEPSP amplitude evolution during induction and maintenance phases of LTP (E-LTP and L-LTP).

Behavioral experiments

In all behavioral test, the corresponding testing apparatus, arena, or object was cleaned with 70% ethanol to remove odors and allowed to dry completely before each animal was tested.

Laboratory animal behavior observation registration and analysis system (LABORAS) behavioral test

To examine potential effects of GIRK modulation on locomotor activity and stress- or anxiety-related behaviors, different behavioral categories (grooming, rearing, climbing, and locomotion) were evaluated with an automated system: LABORAS (Metris B.V.; Fig. 5*A*). Briefly, each animal was placed in a rectangular LABORAS cage [a 23.5 (L) × 17.5 (W) × 4 (H) cm Plexiglas base arena, a 26.5 (L) × 21 (W) × 10 (H) cm top, and a cage lid] 1 h after i.c.v. administration and performed a single 15-min trial. Based on electrical signals resulting from mechanical vibrations generated by the movements of the animals, the time spent moving, grooming, rearing, and climbing was automatically recorded by a sensing platform positioned under the cage. Grooming behavior was used as a measurement of stress-related behavior (Kalueff and Tuohimaa, 2004). Locomotion, climbing, and rearing behaviors were used as measurements of locomotor activity (Buttner, 1991). All data were digitized and analyzed using Metris software.

LABORAS locomotion test

Locomotor activity was further assessed with the LABORAS system by exposure of the animals to an open field (OF) consisting of a LABORAS cage made with a 38 (L) × 22.5 (W) × 4 (H) cm Plexiglas base arena and a 43.5 (L) × 27.5 (W) × 22.5 (H) cm top (Fig. 5*C*). Then, 1 h after i.c.v. injections, mice were placed in the center of the OF arena and allowed to explore freely during a single 15-min trial. Total traveled distance was

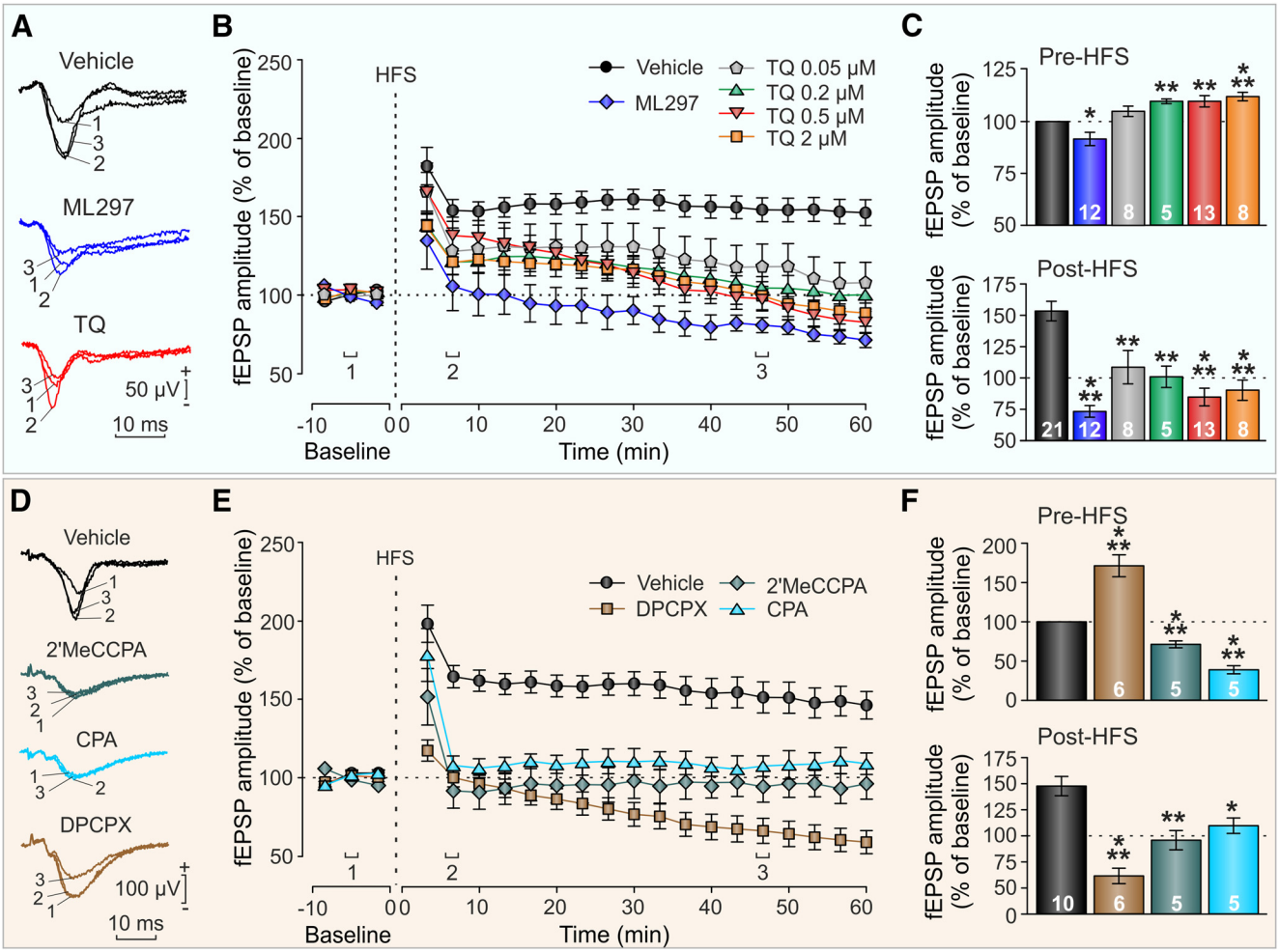

Figure 3. The modulation of GIRK channel activity impairs LTP in the hippocampus through a G-protein-dependent mechanism. ***A***, Representative averaged ($n = 20$) traces of fEPSPs recorded in the CA1 area by stimulation collected before HFS (1; BL), 6 min after HFS (2), and ~46 min after HFS (3) in vehicle, ML297-treated (10 μM), and TQ-treated (0.5 μM) slices. ***B***, Time course of LTP evoked in the CA1 area after an HFS in controls (vehicle), ML297 (10 μM), and different TQ concentrations (0.05–2 μM). ***C***, fEPSP amplitude during BL before HFS (upper bar plot), and the potentiation level in the last 10 min after HFS (bottom bar plot). ***D***, Representative examples of averaged ($n = 20$) fEPSPs evoked before HFS (1; BL), 6 min after HFS (2), and ~46 min after HFS (3) in slices perfused with vehicle, adenosine A_1 receptor agonists 2′MeCCPA (1 μM) and CPA (1 μM), and antagonist DPCPX (100 nM). ***E***, Plot representing evolution of fEPSP amplitude following an HFS in vehicle-treated, 2′MeCCPA-treated, CPA-treated, and DPCPX-treated slices. ***F***, For each experimental group, bars illustrate fEPSP amplitude during BL before HFS (upper bar plot) and the potentiation level in the last 10 min after HFS (bottom bar plot). The number of slices for each condition is indicated on the corresponding bar in ***C***, ***F***. Mean ± SEM is represented. Differences with respect to vehicle (control) are expressed as $*p < 0.05$, $**p < 0.01$, $***p < 0.001$. %, percentage.

automatically tracked and recorded by sensing platforms based on detecting vibrations of the movements of each mouse. All data were digitized and analyzed using Metris software.

Elevated plus maze

The elevated plus maze is a standard ethological-based test of anxiety-related behavior in rodents that enables the assessment of anxiogenic or anxiolytic effects of a treatment by measuring approach-avoidance behavior (La-Vu et al., 2020). Increased percent time and entries into the enclosed arms of the maze are interpreted as greater avoidance of potentially harmful, elevated, open spaces (Walf and Frye, 2007). The test can also be used to determine locomotor activity (Lopes et al., 2021). Here, the test was conducted to further examine both aspects. The maze (LE 842, Panlab S.L.U.) consisted of a cross-shaped methacrylate platform with two open arms without walls and two arms enclosed by 15-cm-high opaque walls, mounted at 90° to one another. Each arm was 65 (L) × 6 (W) cm, and the four arms were separated by a central square of 6.3 - × 6.3 cm. The structure was raised at 40 cm above the floor (Fig. 5*D*). Briefly, 1 h after i.c.v. injections, mice were introduced into the center of the maze facing an open arm and allowed to freely explore the platform during a single 5-min session. Total number of entries into the four arms (total arm entries) and number of entries into the closed arm (closed arm entries) were counted as a measurement of locomotor activity. The number of entries into the open arms (open arm entries) and the percentage of time spent in open arms were used as measurements of anxiety-like behavior.

Rotarod performance task

General motor function and coordination were evaluated using a rotarod apparatus (LE 8500, Panlab S.L.U.) with automatic timers and falling sensors (Fig. 5*B*). Mice were placed on a 30 mm diameter black-striated rod positioned 20 cm above the floor. First, animals were trained until they could stay on the rod for 1 min at constant low-speed (6 rpm) rotation. Then, 24 h later, and 1 h after i.c.v. injections, mice were tested in five consecutive trials. In each trial, the rotarod was set to accelerate from 4 to 40 rpm over a 2-min period (cutoff time) and the latency to fall off the rod was recorded automatically.

OF habituation task

Habituation to a novel environment in rodents is a type of non-associative hippocampal-dependent learning that can be measured as a change in exploration or in locomotor activity after re-exposure (Platel and Porsolt, 1982; Leussis and Bolivar, 2006). In the present work, to test this form of learning and its relation to hippocampal GIRK signaling, mice

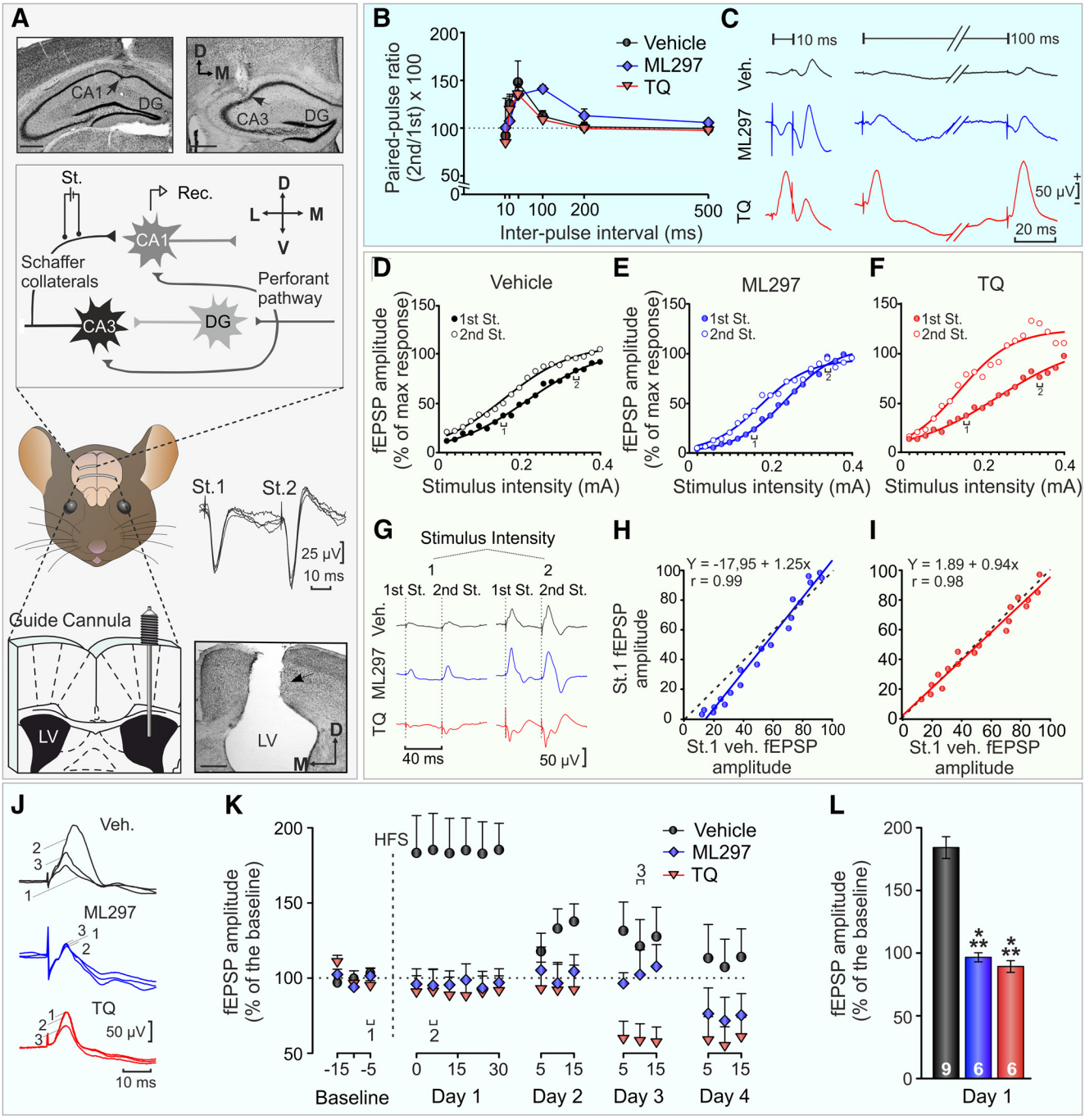

Figure 4. *In vivo* GIRK activity modulation disrupted CA3—CA1 synaptic properties. ***A***, Mice preparation for *in vivo* chronic recording of fEPSPs evoked at the hippocampal CA3—CA1 synapse and i.c.v. drug administration. In the upper half, schema illustrates the location of the implanted recording (Rec.) and stimulating (St.) electrodes. Top photomicrographs show histologic verification of electrode position (indicated with black arrows). In the lower half, on the right, fEPSP profile evoked by paired pulses collected from a representative animal at intermediate stimulus intensities. Bottom left, a stainless-steel guide cannula was implanted, in the left ventricle, contralaterally to both electrodes. Bottom right photomicrograph serves as histologic verification of cannula position (black arrow). Scale bars: 500 μm. LV, lateral ventricle; DG, dentate gyrus; St., stimulus; D, dorsal; M, medial; V, ventral; L, lateral. ***B***, *In vivo* PPF curve at the CA1—CA3 synapse for mice injected i.c.v. with vehicle, ML297, and TQ. PPF was evoked by stimulating Schaffer collaterals at fixed current intensity. Averaged (five times) fEPSP paired traces for each experimental group were collected at interstimulus intervals of 10–500 ms. Data are expressed as mean ± SEM amplitude of the second fEPSP expressed as a percentage of the first [(second/first) × 100] for each of the six interstimulus intervals used in this test (PPR). ***C***, Representative examples (averaged ≥5 times) of fEPSPs evoked at the CA3—CA1 synapse at two different interstimulus intervals (10 and 100 ms) for each experimental group. ***D–F***, I/O curves at the CA3–CA1 synapse for mice i.c.v. injected with vehicle, ML297, and TQ, respectively, were conducted with double pulses of increasing intensity at fixed interstimulus interval (40 ms). max, maximum; % percentage. ***G***, Representative averaged ($n = 5$) records of fEPSPs recorded in the CA1 area following paired-pulse stimulation of the ipsilateral Schaffer collaterals at two different intensities (1, 0.16 mA and 2, 0.34 mA). ***H***, ***I***, Scatter plots illustrating values of fEPSPs evoked by the first pulse in all experimental groups (*x*-axis, vehicle; *y*-axis, experimental group). The best linear fit is illustrated. ***J–L***, Evolution of fEPSPs evoked in the CA1 area by stimulation of Schaffer collaterals after an HFS session in freely moving mice. ***J***, Illustrated traces are representative examples of fEPSPs (averaged ≥5 times) collected from selected i.c.v. vehicle-injected, ML297-injected, or TQ-injected mice evoked by pulses presented to the CA3—CA1 synapse. fEPSPs were collected before (BL) and after the HFS of Schaffer collaterals at the indicated times (see 1, 2, and 3 on the *x*-axis of ***K***). The number of animals for each experimental group is indicated on the corresponding bar (***L***). Mean ± SEM is represented in ***K***, ***L***; ***$p < 0.001$. veh., vehicle.

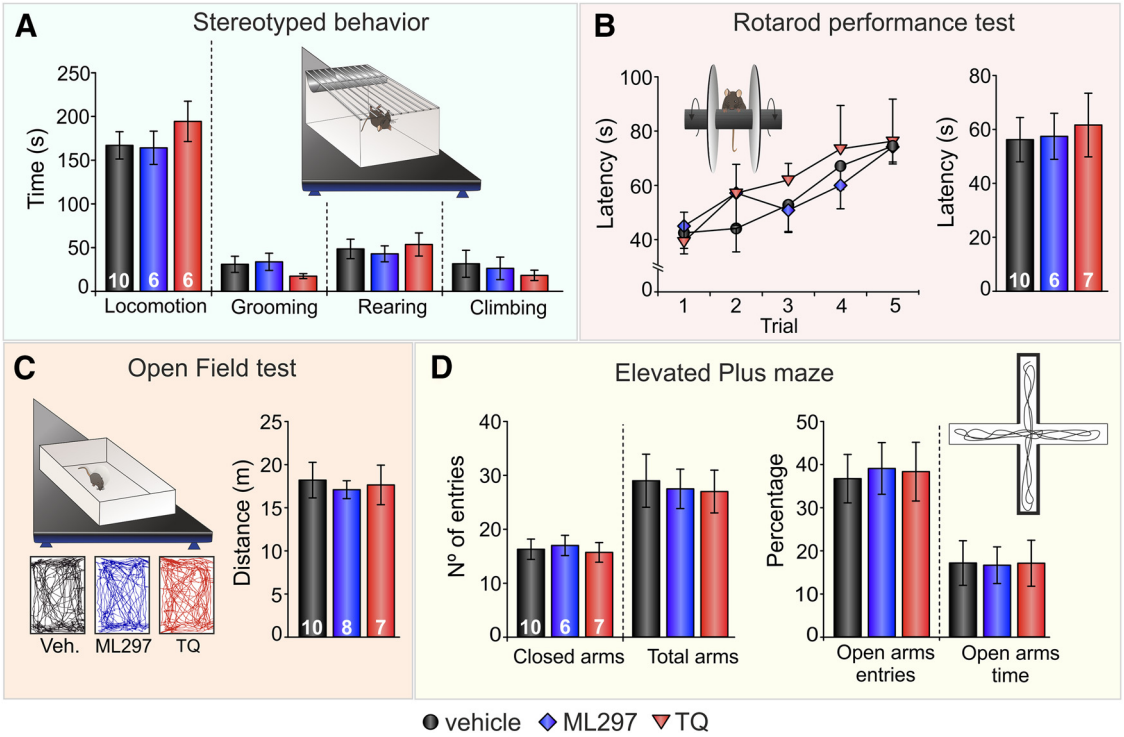

Figure 5. GIRK modulation does not induce alterations in locomotor activity, nor anxiety or depression-like behavior. ***A–D***, Behavioral testing was carried 1 h after i.c.v. injections of vehicle, ML297, or TQ. The number of animals for each experimental group is indicated on the corresponding bar. ***A***, Stereotyped behaviors were assessed using a LABORAS system on the basis of detecting the vibrations generated by the animals. Mice underwent a single 15-min LABORAS session. The bars show the amount of time spent by the animals in each type of activity (locomotion, grooming, rearing, and climbing). ***B***, Rotarod performance test. Locomotor activity was examined 1 h after i.c.v. injections, when animals performed a single session consisting of five trials. Mean latency to fall off the rod was quantified for each trial (left) and the whole session (right). ***C***, OF test. Locomotor activity was further determined with the LABORAS system by measuring the total distance traveled in an OF arena during a single 15-min session. ***D***, Elevated plus maze. After i.c.v. injections, mice were exposed to the platform for 5 min. Locomotion was analyzed by counting the number of entries in closed and total arms. Anxiety levels were assessed by measuring the percentage of entries and percentage of time spent on open arms. Data are represented as mean ± SEM.

were exposed twice to an OF habituation task as described elsewhere (Sánchez-Rodríguez et al., 2020). Briefly, animals performed two consecutive trials (one trial per day): training and habituation (or retention) trials on days 1 and 2, respectively (Fig. 6*A*). During the training trial, mice were initially exposed to the OF. Then, 24 h later, habituation was tested (retention or habituation trial) by re-exposure of the animals to the same OF. Drug concentrations used for i.c.v. injections have been shown not to affect motor activity in mice (Sánchez-Rodríguez et al., 2020; Fig. 5). Exploratory behavior was tested using an actimeter (AC-5, Cibertec), consisting of an infrared system to detect animal movements in a square white acrylic box (35 × 35 × 25 cm). In each trial, mice were placed at random in one of the four corners of the box and allowed to explore it for 15 min. Horizontal (*x*- and *y*-axes crossing summation), vertical (*z*-axis crossing), and total (*x*-, *y*-, and *z*-axes crossing summation) movements were recorded. Recorded data were analyzed using MUX_XYZ16L software (Cibertec).

Novel object recognition (NOR) task

In behaving mice, CA3–CA1 synaptic functionality account for OR memory formation (Clarke et al., 2010). Therefore, to further study the role of GIRK channels on hippocampal-dependent learning, a NOR task was conducted to test recognition memory. The task is based on the preference of mice for exploring a NO over a familiar one, thereby indicating memory of the familiar object previously explored. Here, NOR was tested in a uniformly illuminated OF arena (30 × 40 × 40 cm) and performed on three consecutive days (Fig. 6*B*) as previously described (Sánchez-Rodríguez et al., 2017). Briefly, on day 1, three trials of habituation to the empty arena were performed (5-min trials, separated by 1.5-h resting periods). On day 2, two identical objects were placed in the center of the arena and animals were allowed to explore for 10 min (acquisition/training session). Both 3 and 24 h later, one object was replaced by a new one to perform two 10 min test sessions (NOR1 and NOR2 sessions, see details below) to test short-term memory (STM) and long-term memory (LTM), respectively (Clarke et al., 2010; Sánchez-Rodríguez et al., 2017). New objects were different in shape and color but made of the same material (plastic) and with similar general dimensions. New objects and positioning of new objects were counterbalanced through all experiments to avoid bias. For assessment of STM retention and to determine whether subjects were able to learn the NOR task and to properly consolidate and retrieve OR memory, exploratory behavior toward familiar and NOs was quantified (NOR1 test). Only data from animals that performed successfully (≈94% of subjects) during NOR1, i.e., explored the new object for longer than the familiar one, were analyzed and included in the NOR2 test. To test LTM retrieval 24 h after the training session, the NO used in NOR1 was again replaced by a new novel one. Exploratory behavior toward novel and familiar objects was again measured. To analyze the impact of GIRK channel activity modulation on LTM retention, i.c.v. injections of either vehicle, TQ, or ML297 were performed 1 h before the NOR2 test as described above. Memory was determined by quantifying the relative exploration time for each object and calculating a discrimination index (DI), defined as the difference in exploration time between the two objects, O1 and O2 (TO1 and TO2, respectively), divided by the total time spent exploring the two objects: (TO1 − TO2)/(TO1 + TO2). If we consider O1 to be the NO, a DI >0 will indicate exploration preference for such object.

Sessions were video recorded using a camera placed above the arena. Object exploration was scored by an experienced observer considering exploration only when the subject pointed its nose at a given object at a distance ≤1 cm and/or touched/sniffed the object. When the subject used the object to prop itself up to explore the environment or accidently touched the object while heading in another direction the behavior was not computed as object exploration.

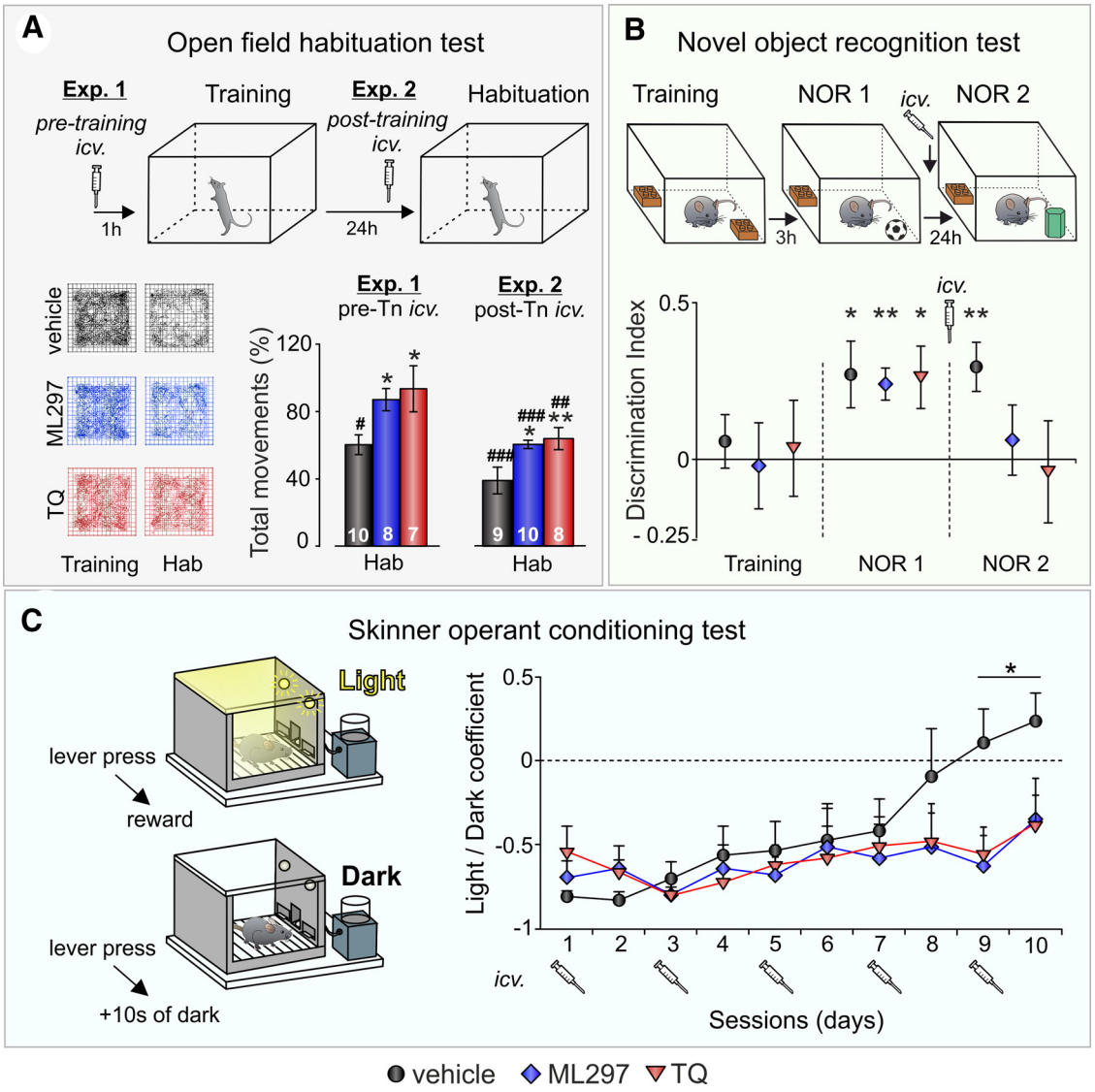

Figure 6. GIRK modulation alters non-associative and associative learning. Experimental design for OF habituation (***A***), NOR (***B***), and Skinner operant conditioning tasks (***C***) are represented in ***A–C***. ***A***, Two sets of experiments were conducted in which i.c.v. injections were performed 1 h before the training session (experiment 1; pre-Tn, pretraining) or habituation session (experiment 2; post-Tn, posttraining). Left bottom panels show examples of mice movement tracking during training and habituation (Hab) sessions for vehicle (control; in black), ML297 (in blue), and TQ (in red) posttraining i.c.v. injections. Histogram represents total activity of each experimental group during habituation session expressed as percentage of exploration during training (100%). The number of animals for each experimental group is indicated on the corresponding bar. ***B***, The NOR test consisted of one training and two NOR testing sessions. During training two identical objects (yellow Lego pieces) were placed in the arena and animals explored for 5 min. After 3 h, one object was replaced by a new one (mini-football ball) for the first test session (NOR1). After 24 h, a second test (NOR2) was conducted with the familiar object and a new novel one (green cylinder). Animals were i.c.v. injected with vehicle, ML297, or TQ 1 h before NOR2 testing. The DI represents the difference between time spent exploring novel and familiar objects. ***C***, Mice were trained in a Skinner box to press a lever to obtain condensed milk as a reward with a FR (1:1) schedule. Animals were trained with two programs of increasing difficulty. First, they had to acquire a FR (1:1) schedule until obtaining the reward, as a criterion, $\geq$20 times in two successive sessions. Afterward, animals were transferred to a L/D paradigm in which lever presses were reinforced only when a light bulb was switched on. Lever presses performed during the dark period delayed the start of the lighted period for 10 s. A L/D coefficient (*y*-axis) was calculated as follows: (number of lever presses during the lighted period − number of lever presses during the dark period)/total number of lever presses; i.c.v. injections were conducted in odd-number sessions. ***A–C***, Data represent mean ± SEM, $*p < 0.05$, $**p < 0.01$ [differences vs vehicle (control) habituation], $\#\#p < 0.01$, $\#\#\#p < 0.001$ (differences vs training).

Operant conditioning task

Operant conditioning is a type of instrumental associative learning involving the activity of many cortical circuits, including the hippocampus (Jurado-Parras et al., 2016). In the present work we checked whether GIRK activity modulation could affect acquisition of an associative learning task. Operant conditioning was conducted in two steps (Fig. 6*C*): a training phase and a L/D test as previously described (Hasan et al., 2013). Both training and testing took place in a Skinner box (20.5 - × 19.5 × 22.5 cm) located inside a sound-attenuating chamber (46 - × 71.5 × 43 cm; Campden Instruments). The operant chamber was equipped with a house light, two levers on the opposite wall with two lights above them, a feeder module between the two levers, and a liquid dispenser coupled to a pump that could deliver 10% condensed milk by lever pressing. Before training, mice were handled daily for 7 d and food-deprived to obtain a weight 85–90% of their free-feeding weight. Training sessions of 20 min were conducted on successive days. Animals were trained, using a fixed-ratio (FR 1:1) schedule, to press a lever to receive 20-µl drops of condensed milk from the liquid dispenser. Turning the house light on and off signaled each session's start and finish, respectively. Mice were maintained on this 1:1 schedule until they reached criterion: pressing the lever $\geq$20 times/session in two successive sessions. Criterion was typically reached after five to seven daily sessions.

Mice that reached training phase (fixed ratio 1:1) criterion were further conditioned using a L/D protocol. In the L/D test animals were

placed in the box for a maximum of 20 min in alternate periods of light and darkness each of 20 s. Only lever presses performed during the light period were reinforced with the liquid reward (success). In contrast, lever presses during the dark period were not rewarded (failure) and extended the period by 10 further seconds. As this complex operant conditioning has been shown to rely on cortical regions additional to the hippocampus (Fernández-Lamo et al., 2018), and learning needs many sessions to be acquired, we decided to administer the drugs sparingly along the test; i.c.v. injections of vehicle, TQ, or ML297 were performed on alternate days of the L/D protocol (starting with session 1) 1 h before the session began. The L/D protocol lasted 10 d including one session/day/animal. In this test, the animal had to press the lever at least a number of times during the light (successes) and the dark (failures) periods ($L/D \geq 0$) for two successive sessions to complete the task (criterion). Animals were allowed a maximum of 10 d to reach criterion. The L/D coefficient [L/D coefficient = (number of lever presses during the light period – number of lever presses during the dark period)/total number of lever presses)] was calculated to determine the learning rate for each animal. Mice did not exhibit any motivational changes or motor deficits that could influence performance before the training phase or because of repeated i.c.v. injections of either ML297 or TQ during L/D testing. Conditioning programs, lever presses, and delivered reinforcements were controlled and recorded by a computer, using ABET II Software (Campden Instruments).

Histology and immunohistochemistry

As indicated above, the prototypical neural GIRK channels in the hippocampus are GIRK1/GIRK2 heteromultimers (Luján et al., 2014). To study the level of expression of both GIRK subunits in the dorsal hippocampus, at the end of either OF habituation test (experiment 1) or operant conditioning experiments in the Skinner box, mice were deeply anesthetized with ketamine/xylazine administered intraperitoneally (75/10 mg/kg; KETALAR, Pfizer and ROMPUM, Bayer) and perfused transcardially with 0.9% saline followed by 4% paraformaldehyde in PBS (0.1 M, pH 7.4). This histologic protocol also enabled verifying the proper location of implanted electrodes and cannulas. Mice brains were removed and cryoprotected with 30% sucrose in PB. Coronal sections (40 μm) were obtained with a sliding freezing microtome (Microm HM 450) and stored at −20°C in a solution of 50% glycerol in PBS until used. Sections including implantation sites in the hippocampus were mounted on gelatinized glass slides and stained using the Nissl technique with 0.25% thionine to determine the location of stimulating and recording electrodes and/or the implanted cannula (Fig. 4*A*).

For fluorescence immunohistochemistry, free-floating sections were treated for 45 min with 10% normal donkey serum (NDS; RRID:AB_2810235, Sigma-Aldrich) in Tris-buffered saline (TBS) containing 0.1% Triton X-100 (TBS-T; #T8532, Sigma), and subsequently incubated overnight at room temperature with polyclonal rabbit anti-GIRK1 (1:400; RRID:AB_2571710, Frontier Institute) or polyclonal rabbit anti-GIRK2 (1:500; AB_2040115, Alomone Labs) primary antibodies prepared in TBS-T with 0.05% sodium azide (#S/2360/48, Fisher Scientific) and 5% NDS. The following day, sections were washed with TBS-T (3 × 10 min) and then incubated for 2 h at room temperature with 1:150 dilutions of FITC-conjugated donkey anti-rabbit (RRID:AB_2315776, Jackson ImmunoResearch) in TBS-T. After several washes with TBS (3 × 10 min), the tissue was incubated for 5 min in 0.01% DAPI (#sc-3598, Santa Cruz Biotechnology) in TBS. Finally, sections were washed with TBS (3 × 10 min), mounted on gelatinized glass slides, dehydrated, and coverslipped using a fluorescence mounting medium (#S3023, Dako mounting medium, Agilent).

Image analysis

Images were acquired by confocal microscopy at 10× magnification using a laser scanning microscope (LSM 800, Carl Zeiss). GIRK1 and GIRK2 subunit expression was analyzed with ImageJ software (RRID:SCR_003070, NIH) by measuring the intensity of immunostaining (i.e., optical density) in randomly selected squares of ∼15 × 15 μm through the stratum lacunosum-moleculare (SLM) and the molecular layer of the dentate gyrus (MDG) in the dorsal hippocampus, as described elsewhere (Sánchez-Rodríguez et al., 2020). GIRK channels are mainly expressed in the dendrites of pyramidal neurons in the dorsal hippocampus, preferentially in distal dendrites. Thus, immunolabeling for both GIRK1 and GIRK2 subunits is more noticeable along the SLM and the MDG (Fernández-Alacid et al., 2011). As previously described, potential variations in optic density between experimental groups could be measured more accurately in these two areas, because of the greater range of measurement values. Mean background level was calculated from four different squares located in non-stained areas (i.e., corpus callosum) and subtracted from the measurements. The values of optical density were normalized with respect to the control (vehicle) group values.

Drugs

All chemicals used in this study were purchased from Abcam or Tocris Bioscience and dissolved in DMSO (2'MeCCPA, CPA, selective adenosine A_1R agonists and DPCPX, A_1R antagonist) or PBS (ML297, a selective opener of GIRK1-containing channels, and the GIRK channel blocker Tertiapin-Q (TQ) with the help of a shaker and/or sonicator and warmth. For *ex vivo* experiments, drugs ML297 (10 μM; #ab143564), TQ (0.02 − 0.5 μM; #ab120432), 2'MeCPPA and CPA (1 μM; #2281/10, #ab120398), or DPCPX (100 nM; #ab12396) were dissolved in aCSF and applied by superfusion to the slices at a rate of 3 ml/min (Sánchez-Rodríguez et al., 2020). For i.c.v. injection, drugs were dissolved in vehicle (PBS). For ML297, because of its high hydrophobicity, a 10-ml stock suspension in PBS (1.5 mM; Sánchez-Rodríguez et al., 2017) was obtained, and was sonicated with warmth. A vigorous vortexing was applied just before administration to infuse it as a microsuspension. For the blocker TQ, a 0.25 mM solution was obtained (Sánchez-Rodríguez et al., 2019). In both cases, 3 μl were injected through the guide cannula using a Hamilton syringe at a rate of 0.5 μl/min as described above.

Data collection and analysis

In vitro and *in vivo* recordings were stored digitally on a computer using an analog/digital converter (CED 1401 Plus). Data were analyzed with the Spike 2 program (CED). As synaptic responses were not contaminated by population spikes, the amplitude (i.e., the peak-to-peak value in mV during the rise-time period) of successively evoked fPSPs was computed and stored for later analysis.

All calculations were performed using SPSS version 20 software (RRID:SCR_002865; IBM). When the distribution of the variables was normal, acquired data were analyzed with a two-tailed Student's *t* test or one-way or two-way ANOVA with time and treatment as within-subjects and between-subjects factors respectively, except in I/O experiments in which intensity was the repeated measure), and with a contrast analysis for a further study of significant differences. For repeated measures, two-way ANOVA, Greenhouse–Geisser correction was used and indicated in the text when sphericity was not assumed. For non-parametric data, statistical analysis of between group differences was performed using a Kruskal–Wallis test (χ^2). Statistical significance was set at $p < 0.05$.

Unless otherwise indicated, data are represented as the mean ± SEM. Computed results were processed for graphical purposes using the SigmaPlot 11.0 package (RRID:SCR_003210; Systat Software Inc.). Final figures were prepared using CorelDraw X8 Software (RRID:SCR_014235).

Results

The goal of this work was to clarify the contribution of GIRK channel activity to long-lasting synaptic plasticity phenomena at the CA1−CA3 synapse and related hippocampal-dependent learning and memory processes.

Induction and maintenance of ex vivo LTP in dorsal hippocampus needs GIRK channel activity

We started our study in a classical slice preparation including dorsal hippocampus (Fig. 2*A*), by testing the effect of GIRK activity modulation on the main functional properties of

CA3−CA1 synapse, PPF, I/O, and LTP. First, single-pulse stimulation applied at Schaffer collaterals was adjusted to yield a large fEPSP with a latency of 3.5–4 ms in the CA1 stratum radiatum free of population spikes (Fig. 2*B*). Perfusion of the slice with APV (50 μM; $n = 10$) did not significantly affect the fEPSP, but it was completely abolished by CNQX (10 μM; $n = 10$), verifying that it was essentially mediated by glutamate-activated AMPA-kainate receptors (Fig. 2*B*).

Next, we checked whether PPF (Zucker and Regehr, 2002), a typical short-term plasticity phenomenon, was altered by GIRK channel activity modulation at the Schaffer collaterals−CA1 synapses. This facilitation protocol also enabled assessing the presynaptic functionality and, therefore, changes in neurotransmitter release. We tested slices for enhancement of synaptic transmission evoked by PPF using a wide range of interstimulus intervals (from 10 to 500 ms) at a fixed intensity (~35% of the amount needed for evoking a maximum fEPSP response). As illustrated in Figure 2*C*, modulation of GIRK conductance induced no significant differences at any of the selected (10, 20, 40, 100, 200, and 500 ms) intervals ($F_{(3.7,38.7)} = 0.42$, $p = 0.78$, vehicle, $n = 12$; ML297, $n = 6$; TQ, $n = 6$). In addition, we examined the evolution of the paired-pulse ratio (PPR) at 40-ms interval, with increasing intensities, from 0.02 to 0.4 mA (Fig. 2*D*). No significant differences were found either in the global evolution of PPR at different intensities ($F_{(38,342)} = 0.708$, $p = 0.903$, vehicle, $n = 11$; ML297, $n = 5$; TQ, $n = 5$) or in PPR for each intensity ($p > 0.05$ for all cases). Paired-pulse analysis indicated that short-term plasticity processes and presynaptic vesicle release probability are not affected by GIRK channel activity.

The excitability of the CA3−CA1 synapse was then studied by I/O protocols. The stimulus intensity was increased in steps of 0.02 mA from 0.02 to 0.4 mA, maintaining a fixed 40-ms interval between paired pulses. Increasing intensity of electrical stimulation delivered at Schaffer collaterals was accompanied by greater amplitude of fEPSPs for first ($F_{(19,190)} = 272.159$, $p < 0.001$) and second $F_{(19,190)} = 11.336$, $p < 0.001$) stimulus ($n = 11$; Fig. 2*E*,*H*). Slices perfused with ML297 showed a significant decrease of fEPSPs evoked by the second pulse ($n = 5$; $F_{(19,266)} = 3.371$, $p < 0.001$; Fig. 2*F*), whereas those perfused with TQ presented an increase for the response evoked by the second stimulus ($n = 5$; $F_{(19,266)} = 4.318$, $p < 0.001$; Fig. 1*G*). The scatter plots in Figure 2*I*,*J* compare fEPSP amplitudes for the first pulse collected from slices treated with vehicle during the I/O study (on the *x-axis*) with the corresponding values for ML297 or TQ perfusion (*y-axis*). Data were shifted and presented a linear slope > 1 ($b = 1.11$) for ML297 consistent with a decreased excitability, while data for TQ fitted a value ≈ 1 ($b = 0.99$), suggesting that any tendency to increase synapse excitability could be damped.

As we found GIRK channels to modulate CA3−CA1 synapse excitability, before LTP induction, basal fEPSP amplitude was monitored during the perfusion of specific GIRK drugs (Fig. 3*A*–*C*). The amplitude of synaptic responses was decreased by ML297 ($t_{(35)} = 2.56$, $p = 0.015$; Fig. 3*B*,*C*), whereas TQ significantly increased fEPSP amplitude except for the lowest concentration (0.05 μM, $t_{(23)} = -1.54$, $p = 0.14$; 0.2 μM, $t_{(14)} = -4.13$, $p = 0.01$; 0.5 μM, $t_{(38)} = -3.39$, $p = 0.002$; 2 μM; $t_{(23)} = -5.36$, $p < 0.001$; Fig. 3*B*,*C*). Then, after BL was established, we examined the effects of GIRK modulation on synaptic plasticity. HFS applied at Schaffer collaterals induced a robust synaptic potentiation at the CA3–CA1 synapses in control hippocampal slices, which remained stable for at least 1 h (156 ± 1.7%, $n = 21$; $F_{(1.1,22)} = 44.3$ Greenhouse–Geisser correction, $p < 0.001$ vs BL; Fig. 3*B*). However, the presence of the GIRK1-containing channels opener ML297 (10 μM) blocked LTP induction (73 ± 2.6%, $n = 12$; $F_{(1.2,13.5)} = 32.3$ Greenhouse–Geisser correction, $p < 0.001$; Fig. 3*A*–*C*) even causing an LTD (*post hoc* vs BL $p < 0.001$; Fig. 3*B*,*C*). Interestingly, LTP was also induced, although with less amplitude than in controls, and maintained during 30 min after HFS at different TQ concentrations (0.05 μM, $n = 8$, 130 ± 5%, $F_{(10,70)} = 3.99$, $p < 0.001$; 0.2 μM, $n = 5$, 122 ± 1.8%, $F_{(10,40)} = 8.36$, $p < 0.001$; 0.5 μM, $n = 13$, 127 ± 3.3%, $F_{(1.6,18.8)} = 7.28$ Greenhouse–Geisser correction, $p = 0.007$; 2 μM, $n = 8$, 120 ± 2.7%, $F_{(10,70)} = 5.39$, $p < 0.001$; Fig. 3*A*–*C*). However, 30 min after induction none of these potentiations could be maintained (Fig. 3*B*) and they disappeared ~50 min post-HFS (last 10 min post-HFS vs BL, $F_{(5,61)} = 16.08$, $p < 0.001$; *post hoc* 0.05 μM, $p = 0.002$; 0.2 μM, $p = 0.003$; 0.5 μM, $p < 0.001$; 2 μM, $p < 0.001$; Fig. 3*C*), even reaching values of synaptic depression for 0.5 μM.

It has previously been shown that a fraction of basal GIRK activity consists of G-protein-independent component (Rishal et al., 2005). However, in the dorsal hippocampus, adenosine A_1 receptors seem to mediate basal GIRK activity by a G-protein-dependent mechanism (Kim and Johnston, 2015; Reis et al., 2019; Jeremic et al., 2021). Thus, we wanted to clarify the G-protein dependence of the GIRK conductance in the CA3−CA1 synapse. First, before application of the HFS protocol, we explored the effects of A_1 receptor selective modulation on basal amplitude of synaptic responses (Fig. 3*D*,*F*). A_1 receptor activation with both agonists, 2'MeCCPA or CPA, significantly reduced the amplitude of recorded fEPSPs (2'MeCCPA, $n = 5$, $t_{(14)} = 6.732$, $p < 0.001$; CPA, $n = 5$, $t_{(14)} = 9.703$, $p < 0.001$), while after receptor block with DPCPX, synaptic response amplitude was considerably increased ($n = 6$, $t_{(17)} = -5.145$, $p < 0.001$; Fig. 3*D*,*F*). Then, once BL was stabilized, we checked the effects of slice perfusion with A_1 selective modulators on synaptic plasticity (Fig. 3*E*,*F*). The potentiation protocol did ensure LTP induction in control slices ($n = 10$, 160 ± 2.4%, $F_{(10,90)} = 50.428$, $p < 0.001$). However, when 2'MeCCPA and CPA were perfused, LTP induction was completely abolished after potentiation protocol application (2'MeCCPA, 95 ± 3.5%, $F_{(10,40)} = 0.598$, $p = 0.806$; CPA, 109 ± 2.1%, $F_{(10,40)} = 1.399$, $p = 0.216$). In contrast, application of DPCX, besides preventing the induction of LTP, significantly depressed the amplitude of synaptic responses, thereby causing LTD (61 ± 4.1%, $F_{(1.1,5.7)} = 22.280$, $p = 0.003$; Fig. 3*E*,*F*).

Hence, our results suggest that A_1 receptor activity generates an optimal range of GIRK conductance required for LTP induction and maintenance, and receptor or channel malfunction creates an alteration that disturbs this critical form of plasticity in the dorsal hippocampus.

In vivo LTP in the dorsal hippocampus requires CA3−CA1 excitability regulation exerted by GIRK channels

Long-term synaptic plasticity phenomena (LTP/LTD) that take place in the dorsal hippocampus have been shown to primarily perform cognitive functions (Fanselow and Dong, 2010). The induction threshold for LTP/LTD depends on hippocampal excitability level (Lüscher and Malenka, 2012; Keck et al., 2017), controlled, in part, by GIRK channels (Lüscher and Slesinger, 2010; Jeremic et al., 2021), as we also found here *ex vivo*. Therefore, before studying the impact of channel modulation on hippocampal-dependent learning and memory functions in mice, the next step was to investigate *in vivo* the role of GIRK activity in hippocampal CA3−CA1 excitability and subsequently, in short-lasting and long-lasting synaptic plasticity changes. To address this question, we took advantage of *in vivo* recording techniques and studied functional properties of the dorsal

CA3−CA1 hippocampal synapse by I/O, PPF, and LTP protocols in behaving mice (Fig. 4).

To study CA3−CA1 excitability, the I/O protocol consisted of paired electrical stimuli with an interval of 40 ms and increasing intensity (range 0.02–0.4 mA in steps of 0.02 mA), applied at Schaffer collaterals to evoke a large fEPSP in the CA1 pyramidal cells (Fig. 4*A*,*G*). fEPSPs from control animals showed the characteristic increasing sigmoid-like curve for the first ($F_{(19,247)}$ = 58.68, $p < 0.001$) and second ($F_{(19,247)}$ = 19.35, $p < 0.001$) stimulus (Fig. 4*D*,*G*). The evolution of the first and second fEPSPs evoked by the same pair of pulses at the same range of intensities (0.02–0.4 mA) was not significantly different for mice injected with ML297 (Fig. 4*E*,*G*) or TQ (Fig. 4*F*,*G*). Excitability of the CA3−CA1 pathway was evaluated by plotting values of fEPSPs evoked by the first pulse in experimental groups (*y*-axis) against control values (*x*-axis; Gruart et al., 2012). As we also found *ex vivo*, for the ML297 group, values were shifted downward, and the slope of the linear fits were >1 ($b = 1.25$), in accordance with a decrease in excitability (Fig. 4*H*), while for the TQ group, the slope was <1 ($b = 0.94$) and values were shifted upward, suggesting a slight increase in excitability (Gruart et al., 2012; Sánchez-Rodríguez et al., 2017; Fig. 4*I*).

Next, functional capabilities of the CA3–CA1 synapse were studied by checking a typical short-term plasticity phenomenon of this synapse: the PPF (Fig. 4*B*,*C*). Mice were tested for enhancement of synaptic transmission evoked by PPF using a wide range of interstimulus intervals (from 10 to 500 ms) at a fixed intensity (≈35% of the amount needed for evoking a maximum fEPSP response). As illustrated in Figure 4*B*, all groups presented a significant ($F_{(2.75,77.06)}$ = 5.30, Greenhouse–Geisser correction, $p = 0.003$) increase of the response to the second pulse at short (40–100 ms) time intervals. No significant differences between groups were observed at any of the selected intervals ($F_{(2,28)}$ = 1.02, $p = 0.37$), thus suggesting not only a normal short-term hippocampal plasticity but also that the drugs used in the present work are preferentially acting at postsynaptic locations, as we found *ex vivo*.

As neural excitability level regulates the induction threshold for LTP/LTD (Keck et al., 2017) and we observed LTP to be transformed into LTD *ex vivo* when GIRK conductance was modified, we asked whether modulation of the GIRK-dependent signaling by i.c.v. injections would impair *in vivo* synaptic plasticity in a similar manner. HFS applied at CA3 Schaffer collaterals induced a significantly enhanced fEPSP amplitude in the stratum radiatum of dorsal CA1 (184 ± 9% of BL; $n = 9$; Fig. 4*J*–*L*) during the 30 min following HFS ($F_{(1.43,11.42)}$ = 12.08, $p = 0.003$). However, LTP could not be induced when GIRK channel activity was pharmacologically enhanced or reduced through i.c.v. injections (ML297, $F_{(8,40)}$ = 0.3, $p = 0.963$, $n = 6$; TQ, $F_{(8,40)}$ = 0.924, $p = 0.508$, $n = 6$; Fig. 4*J*–*L*). Interestingly, both modulations induced a depression of the synaptic response that was noticeable in ML-injected (75 ± 8% of BL) and TQ-injected (58 ± 6% of BL) animals 72 and 48 h after HFS, respectively (Fig. 4*K*). These results suggest that activity of GIRK channels is critical for the induction and maintenance of synaptic plasticity processes in the dorsal hippocampal CA3−CA1 synapse.

Motor function, coordination, and emotional state after *in vivo* GIRK modulation

Before testing electrophysiological findings in learning and memory tasks, we wanted to rule out the possibility that the results might be biased by motor impairments or changes in emotional state triggered by the drugs used in this study. A battery of behavioral tasks was conducted to assess motor function, stress, and anxiety levels of i.c.v.-injected animals. First, mice (vehicle, $n = 10$; ML297, $n = 6$; TQ, $n = 6$) were challenged in the automated system *LABORAS* to measure the amount of time spent performing different predefined behavioral activities. As it can be observed in Figure 5*A*, no differences between groups were found for any of the behavioral categories analyzed: grooming ($F_{(2,19)}$ = 0.846, $p = 0.445$), locomotion ($F_{(2,19)}$ = 0.694, $p = 0.512$), rearing ($F_{(2,19)}$ = 0.172, $p = 0.843$), and climbing ($\chi^2_{(2)}$ = 0.206, $p = 0.902$). These results suggest that motor function and stress or anxiety levels are not affected by pharmacological modulation of GIRK channels. To further examine locomotor activity animals were also challenged in the rotarod performance task (Fig. 5*B*). Our data showed that mice improved their performance across trials regardless of the treatment [vehicle ($n = 10$), $F_{(4,36)}$ = 3.864, $p = 0.01$; ML297 ($n = 6$), $F_{(4,20)}$ = 3.238, $p = 0.033$; TQ ($n = 7$), $F_{(4,24)}$ = 3.554, $p = 0.021$], without differences between groups ($F_{(2,20)}$ = 0.152, $p = 0.86$), indicating that motor function and coordination were preserved. Consistent with these findings, the distance traveled by the animals in a LABORAS locomotion test performed in an OF was similar for all groups (vehicle, $n = 8$; ML297, $n = 6$; TQ, $n = 6$; $F_{(2,17)}$ = 0.175, $p = 0.841$; Fig. 5*C*). Finally, both locomotor activity and anxiety levels were evaluated in an elevated plus maze (Fig. 5*D*). As expected, all experimental groups (vehicle, $n = 8$; ML297, $n = 6$; TQ, $n = 6$) exhibited a similar number of entries in closed arms ($F_{(2,17)}$ = 0.083, $p = 0.921$) and total arms ($F_{(2,17)}$ = 0.426, $p = 0.66$), corroborating our previous results related to motor function. More remarkably, no differences were found in the percentage of entries ($F_{(2,17)}$ = 0.818, $p = 0.458$) or time ($F_{(2,17)}$ = 1.225, $p = 0.318$) spent in the open arms, providing evidence that GIRK modulation through i.c.v. injections was not associated with abnormal anxiety levels.

GIRK activity modulation impairs non-associative and recognition hippocampal-dependent learning

Our electrophysiological results *ex vivo* and *in vivo* strongly suggested that GIRK activity was essential to control both excitability of the CA3−CA1 synapse and induction and maintenance of plastic mechanisms involved in all different stages of memory processing (memory formation, storage, and retrieval). Many associative and non-associative learning and memory tasks have been shown to depend substantially on CA3−CA1 dorsal hippocampus functionality (Gruart et al., 2006; Gruart and Delgado-García, 2007; Clarke et al., 2010; Fernández et al., 2017). So, we then wanted to assess the contribution of GIRK channel activity, by i.c.v. injections and behavioral testing.

First, we challenged our experimental groups on the OF habituation test. Two different experiments were designed in two different cohorts of mice to assess distinct phases of habituation memory processing. *Icv.* injections were performed either before (experiment 1; pretraining i.c.v.) or after (experiment 2; posttraining i.c.v.) the acquisition trial (training; Fig. 6*A*). In the training session, experimental groups showed no significant differences in exploratory activity regardless the protocol followed for i.c.v. injection (Fig. 6*A*). However, because of the habituation process, animals that received pretraining or posttraining injections of vehicle exhibited a decrease of the exploratory movements on the retention day indicating proper retrieval of habituation memory (habituation trial; Fig. 6*A*, experiment 1; pretraining injections of vehicle, $n = 10$, $t_{(9)} = 2.39$, $p = 0.041$; posttraining injections of vehicle, $n = 9$, $t_{(8)} = 7.22$, $p < 0.001$). However, animals that received posttraining injections of ML297

or TQ reduced their movements during the retention day [ML297 ($n = 10$): $t_{(9)} = 11.27$; $p < 0.001$; TQ ($n = 8$): $t_{(7)} = 4.65$; $p = 0.002$; Fig. 6*A*, experiment 2], but this decrease was less noticeable than that observed in vehicle-injected mice (ML297 vs vehicle: $p = 0.014$, TQ vs vehicle: $p = 0.008$; Fig. 6*A*, experiment 2), suggesting impaired habituation memory retrieval. Similarly, mice injected with ML297 or TQ before the training traveled longer distances (ML297 vs vehicle: $p = 0.032$; TQ vs vehicle: $p = 0.012$) and did not show significant habituation [ML297 ($n = 8$): $t_{(7)} = 1.42$, $p = 0.119$; TQ ($n = 7$), $t_{(6)} = 0.282$, $p = 0.787$; Fig. 6*A*, experiment 1], again suggesting an impaired retrieval. Exploration distance within the training session for animals that received pretraining i.c.v. injections was also analyzed to evaluate intra-session habituation during training that could be related to encoding defects. All animals habituated along the 15-min trial (analysis of consecutive 1-min time blocks; vehicle: $F_{(14,126)} = 11.310$, $p < 0.001$; ML297: $F_{(14,98)} = 14.634$, $p < 0.001$; TQ: $F_{(14,84)} = 4.059$, $p < 0.001$; with no differences between groups $F_{(2,22)} = 0.092$, $p = 0.912$). As all animals explored less at the end of the training session than at the beginning of the trail, but showed impaired retrieval during retention testing, it could be hypothesized that, additionally to retrieval, storage/consolidation processes more likely than encoding, could also be affected by GIRK modulation (Etkin et al., 2006). Together, these results suggest that GIRK channel activity disruption (either an increase or decrease) by i.c.v. injections clearly impairs retrieval of habituation memory, although other phases of memory processing for habituation could also be affected by i.c.v. GIRK modulation.

Additionally, we wanted to investigate the role of GIRK activity in long-term recognition memory retrieval, so we chose the OR memory test as it has been shown to significantly depend on CA3−CA1 synaptic functionality in behaving mice (Clarke et al., 2010). The task relies on the innate curiosity of rodents to explore a NO more than a familiar one. During training (Fig. 6*B*), animals spent a similar amount of time exploring each object, with a DI near to 0 ($p > 0.05$ in all experimental groups; Fig. 6*B*). The NOR1 session was performed 3 h after training, and mice showed a strong preference for exploring the NO [vehicle ($n = 16$): DI = 0.27 ± 0.11, $t_{(15)} = 2.54$, $p = 0.023$; ML297 ($n = 10$): DI = 0.24 ± 0.05, $t_{(9)} = 4.7$, $p = 0.001$; and TQ ($n = 6$): DI = 0.26 ± 0.1, $t_{(5)} = 2.6$, $p = 0.047$], suggesting proper memory formation and STM retrieval for all animals. 24 h later i.c.v. drug injections were performed, and after 1 h, mice underwent a new testing session (NOR2) to assess LTM retrieval. Vehicle-injected mice ($n = 16$) showed DI values similar to those from NOR1, showing again a clear discrimination between novel and familiar objects for these control animals (DI = 0.3 ± 0.08, $t_{(15)} = 3.76$, $p = 0.002$). However, DI values for ML297-i.c.v. injected and TQ-i.c.v. injected mice were not significantly different from training values [ML297 ($n = 8$): DI = 0.06 ± 0.11, $t_{(7)} = 0.55$, $p = 0.602$; and TQ ($n = 6$): DI = -0.04 ± 0.16, $t_{(5)} = -0.25$, $p = 0.82$], indicating that these animals were not able to retrieve the memory for the familiar object and therefore recognize the new objects (Fig. 6*B*).

In summary, these experiments demonstrate that dysregulation of GIRK activity by i.c.v. injections also disrupts retrieval of recognition memory, i.e., impairing LTM processes (habituation and recognition memories) that have being shown to depend on CA3–CA1 hippocampal synapse functionality.

Role of GIRK channels in associative learning: operant conditioning

Finally, as we found GIRK channel activity to be necessary for non-associative hippocampal-dependent memory, we also wanted to assess its involvement in associative learning acquisition and performance. For this purpose, an operant conditioning test was conducted as the hippocampus, among other prefrontal and striatal sites (Gruart et al., 2015), is involved in both acquisition and storage of this type of learning (Jurado-Parras et al., 2016). Mice were first trained in a Skinner box to obtain condensed milk every time they pressed a lever in daily sessions of 20 min (fixed ratio of 1:1, Fig. 6*C*). The criterion of successful completion of the task was 20 lever presses in two successive sessions. After 10 sessions, 87.5% of trained mice completed the task (Fig. 6*C*). Animals that successfully reached criterion (i.e., that were able to successfully learn and perform the task) were challenged to a more complex operant conditioning task designed as a L/D conditioning test with 10 sessions. Pressing the lever was rewarded only during periods of 20 s in which a light bulb located above the lever was switched on (Fig. 6*C*). Then, mice were injected i.c.v. with GIRK drugs (ML297 and TQ) every two sessions (Fig. 6*C*). Statistical analysis of the learning rate (measured by the L/D coefficient) showed that only vehicle-injected mice ($n = 6$) significantly progressed along testing sessions ($F_{(9,45)} = 9.11$, $p < 0.001$). Moreover, from the ninth session, animals injected with vehicle showed significant differences in the L/D coefficient ($F_{(2,16)} = 4.03$, $p = 0.04$) with respect to both ML297-injected ($n = 6$; *post hoc* vs vehicle, $p = 0.03$) and TQ-injected groups ($n = 7$; *post hoc* vs vehicle, $p = 0.03$; Fig. 6*C*), indicating learning success for control mice. Since animals injected with GIRK modulators did not exhibit any motor or motivational impairment (Fig. 5), our findings cannot be attributed to any specific difficulty to move around in the Skinner box or to any evident hyperactivity or motor inactivity (Jurado-Parras et al., 2016). Hence, these data show that altering GIRK channel activity by i.c.v. pharmacological modulation also results in a significant deficit in the ability to learn an associative operant task.

GIRK protein expression in dorsal hippocampus after *in vivo* activity modulation

As GIRK channels are formed by GIRK1/GIRK2 heteromultimers in the hippocampus (Fernández-Alacid et al., 2011), we then asked whether modulation of GIRK channel activity would alter the expression of the two subunits at the protein level. We analyzed the optical density of GIRK1 and GIRK2 subunits in immunostained sections through the SLM and MDG of the dorsal hippocampus. Staining was measured: (1) 24 h after a single i.c.v. injection of either vehicle, ML297, or TQ; (2) after multiple i.c.v. injections (five injections, in alternated days) of the same drugs. Twenty-four hours after a single i.c.v. injection of ML297, the intensity of GIRK1 and GIRK2 staining was similar to that of vehicle-injected animals (Fig. 7*A*,*B*) for both SLM (GIRK1, $n = 15$ slices, $94 \pm 4.63\%$ of control vehicle values, *post hoc* vs control, $p = 0.535$; GIRK2, $n = 16$ slices, $102 \pm 5.77\%$, *post hoc* vs control, $p = 0.985$) and MDG (GIRK1, $n = 16$ slices, $96 \pm 7.26\%$ of control vehicle values, *post hoc* vs control, $p = 0.919$; GIRK2, $n = 16$ slices, $105 \pm 3.58\%$ of control vehicle values, *post hoc* vs control, $p = 0.471$). Likewise, 24 h after a single TQ injection, GIRK1 and GIRK2 optical density remained unaltered in the SLM (GIRK1, $n = 20$ slices, $98 \pm 7.06\%$ of control vehicle values, $p = 0.811$; GIRK2, $n = 19$ slices, $95 \pm 8.34\%$ of control vehicle values, *post hoc* vs control, $p = 0.937$) and MDG (GIRK1, $n = 20$ slices, $96 \pm 7.75\%$ of control vehicle values, *post hoc* vs control, $p = 0.971$; GIRK2, $n = 19$ slices, $106 \pm 5.31\%$ of control vehicle values, *post hoc* vs control, $p = 0.312$). In contrast, our results show that multiple i.c.v. injections of ML297 produced a

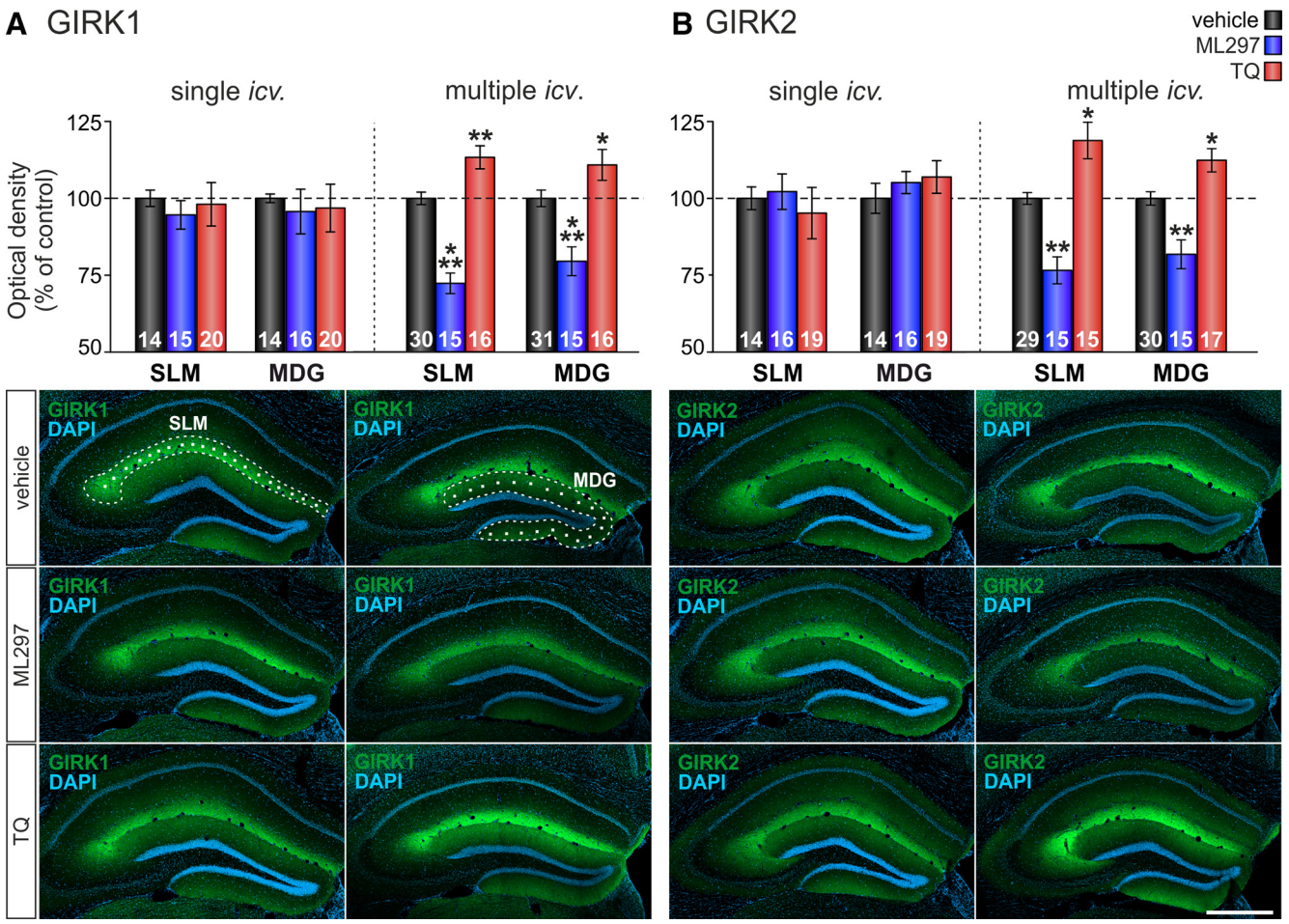

Figure 7. Hippocampal GIRK protein expression pattern after GIRK activity modulation. ***A***, ***B***, Bar plots for single or multiple i.c.v. drug injection showing GIRK1 (***A***) and GIRK2 (***B***) immunostaining intensity (measured as optical density) expressed as percentage of control (vehicle) values (dashed line, 100%) in the SLM and the MDG of the dorsal hippocampus in mice i.c.v. injected with vehicle (control), ML297, or TQ. Number of hippocampal sections for each condition is indicated on the corresponding bar (in animals: single i.c.v.: vehicle, $n = 4$; ML297, $n = 4$; TQ, $n = 5$; multiple i.c.v.: vehicle, $n = 7$; ML297, $n = 4$; TQ, $n = 4$). Differences versus control (vehicle) are indicated by asterisks (*$p < 0.05$, **$p < 0.01$, ***$p < 0.001$). Confocal fluorescence photomicrographs show the distribution of GIRK1 (***A***) and GIRK2 (***B***) subunits (green labeling) and DAPI-stained cells (blue labeling) in the dorsal hippocampus of each representative group. The images in ***A*** (GIRK1-vehicle) illustrate how random 15×15 μm squares were distributed through the SLM (left panel, area within the white dashed line) and MDG (right panel, area within the white dashed line) to measure GIRK1 and GIRK2 optical density. Calibration bar: 500 μm.

significant decrease in GIRK1 and GIRK2 staining (Fig. 7*A*,*B*) in the SLM (GIRK1, $n = 15$ slices, $72 \pm 3.3\%$ of control vehicle values, *post hoc* vs control, $p < 0.001$; GIRK2, $n = 15$ slices, $78 \pm 4.8\%$ of control vehicle values, *post hoc* vs control, $p = 0.0014$) and MDG (GIRK1, $n = 15$ slices, $79 \pm 4.7\%$ of control vehicle values; *post hoc* vs control, $p < 0.001$; GIRK2, $n = 15$, $81 \pm 4.7\%$ of control vehicle values, *post hoc* vs control, $p = 0.006$). On the other hand, multiple TQ i.c.v. injections induced a significant increase in GIRK1 and GIRK2 optical density (Fig. 7*A*,*B*) in both SLM (GIRK1, $n = 16$, $113 \pm 3.8\%$ of control vehicle values, *post hoc* vs control vehicle, $p = 0.0012$; GIRK2, $n = 15$, $120 \pm 5.9\%$ of control vehicle values, *post hoc* vs control, $p = 0.0102$) and MDG (GIRK1, $n = 16$ slices, $110 \pm 5\%$ of control values, *post hoc* vs control vehicle, $p = 0.044$; GIRK2, $n = 17$, $113 \pm 3.6\%$ of control values, *post hoc* vs control vehicle, $p = 0.014$). Pharmacological channel desensitization/sensitization mechanisms could account for these effects (Golan et al., 2016) or mechanisms that might involve modulation of GIRK subunits trafficking (Luján and Aguado, 2015). These results suggest that acute alterations by single pharmacological i.c.v. manipulation of GIRK activity do not modify total channel expression levels on the hippocampus, although there could be different surface or functional expression changes that were not determined by our immunohistochemical approach. In contrast, present results show that sustained and prolonged modulation of GIRK conductance may have a large impact on hippocampal channel protein expression.

In summary, our electrophysiological evidence on excitability and LTP/LTD thresholds impairments supports a direct effect of ML297 and TQ on GIRK channels, by opening and a blockade of the channels, respectively. A compensatory effect on protein expression of sustained activation or blocking of the channel is also found but does not seem responsible for the "net" functional effect exerted by these drugs (as would imply opposite electrophysiological results on excitability levels as the ones presented here).

Together, our results show, for the first time and at different levels of complexity, that GIRK channel activity is required to perform cognitive functions that depend on hippocampal performance.

Discussion

GIRK channel activity, excitability, and synaptic plasticity in CA3–CA1 hippocampal synapse

Our *ex* and *in vivo* results showed an impaired LTP in the dorsal hippocampus when GIRK channel activity is pharmacologically modulated. LTP was blocked when ML297 boosted GIRK

conductance, very likely because of the high resting GIRK conductance in the dorsal hippocampal dendrites, which decreases excitability and increases the threshold for LTP induction (Malik and Johnston, 2017). Moreover, the excess of hyperpolarization owing to GIRK conductance enhancement may be the explanation for the HFS protocol leading to insufficient activation of NMDA receptors (NMDARs) that results in a modest increase in intracellular Ca^{2+} levels, causing a decrease in synaptic efficacy (Cummings et al., 1996). In the CA3−CA1 synapse of behaving mice, LTD has not been possible to evoke by the classical 600 pulses presented at 1 Hz in slices (Bliss et al., 2006; Gruart et al., 2015). However, it can be induced by HFS if the threshold required for LTP induction is not reached (for example by GIRK activity enhancement), according to the Bienenstock, Cooper, and Munro (BCM) theory of synaptic plasticity, which suggests the necessity of a certain threshold for LTP induction (Cooper and Bear, 2012). Hence, modulation of GIRK channel activity may facilitate or compromise both plasticity processes: LTP/LTD. This is an important mechanism to produce changes in the ability to induce subsequent synaptic plasticity under physiological and pathologic conditions, a basic phenomenon for metaplasticity (Abraham, 2008).

We also found that decreasing GIRK conductance with TQ disrupts LTP *ex* and *in vivo*. However, these results revealed significant differences with previous *ex vivo* studies where TQ produced an increase in LTP amplitude (Malik and Johnston, 2017). This discrepancy could be explained by several differences: (1) in our *ex vivo* preparation, the depression of LTP in slices appeared at significantly longer periods (>30 min) than those examined by them (first 30 min); and (2) we recorded fEPSPs from CA1 stratum radiatum, with greater sensitivity to detecting changes in CA3−CA1 parameters (Gruart et al., 2012) than patch-clamping recordings obtained from one pyramidal cell. To verify these results, we performed a dose–response study and confirmed that LTP was always depressed by TQ. The explanation for this phenomenon might be a self-regulation mechanism of GABAergic interneurons that is crucial for the induction of LTP. During HFS, GABA reduces its own release by activating $GABA_B$ autoreceptors (i.e., generating an increase in GIRK activity), which ensures enough NMDAR activation to induce LTP (Davies et al., 1991). As hippocampal GIRK channels may act as effector of $GABA_B$ (Koyrakh et al., 2005), their blockade likely interferes with such regulation process, causing an excess of GABA in the medium, the inhibition of pyramidal neurons, and LTP depression over time. The same situation might also be used to explain our *in vivo* results, because in behaving animals HFS intensity needs to be higher than *ex vivo* to successfully induce LTP (Madroñal et al., 2007); thus, in the presence of TQ, GABA release would be so high that NMDARs cannot properly be activated (Davies et al., 1991), also explaining the HFS-induced LTD (Keck et al., 2017).

The depressive effect of TQ on LTP *ex vivo* showed a slow time course noticeable after 30 min of potentiation, which suggests a differential role over the diverse temporal phases of synaptic plasticity. LTP can temporally and mechanistically be divided mainly into two phases: E-LTP and L-LTP, functionally linked to STM and LTM processes (Bliss et al., 2007; Hardt et al., 2014). Our *ex vivo* data showed that although GIRK activity was decreased by TQ, the synaptic response recorded from CA1 may be potentiated by HFS for at least 30 min. After this E−LTP phase, GIRK activity deficits induced LTP-maintenance mechanisms to fail, and potentiation decayed. The conversion of E-LTP into L-LTP seems to be critical for the STM transformation into LTM (Villarreal et al., 2002). So the increased release of GABA discussed in the previous paragraph might induce a slow LTP suppression (Davies et al., 1991), as has recently been proposed for tonic $GABA_A$ conductance in the hippocampus (Dembitskaya et al., 2020).

However, in the dorsal hippocampus, GIRK channels not only gate glutamatergic LTP (Malik and Johnston, 2017). LTP of GIRK currents has been described (Huang et al., 2005) and recently proposed as a mechanism involved in the extinction of fEPSP potentiation to basal levels to process new synaptic plasticity events and subsequent learning and memory formation, as *in vivo* it appeared 48 h after HFS (Sánchez-Rodríguez et al., 2019). Interestingly, HFS raises GIRK channel surface density by NMDAR activation (Chung et al., 2009), explaining why such long-term inhibitory effects are more noticeable at longer times, when mechanisms needed to initiate L-LTP maintenance are operating (Hardt et al., 2014). In addition, synaptic plasticity can be modified by changing the level of presynaptic and postsynaptic $GABA_B$ and A_1R desensitization via GIRK activity (Wetherington and Lambert, 2002; Reis et al., 2019; Hill et al., 2020). These findings agree with our immunohistochemical findings, as sustained and prolonged changes in the activity of the channel (by multiple i.c.v. injections) may induce compensatory regulations at the protein level by channel sensitization/desensitization or trafficking regulation. On the contrary, acute pharmacological opening/blockage of the channels (by single i.c.v. drug injection) did not seem to induce changes in total protein channel's expression although it cannot be ruled out that unmeasured differential surface or functional expression might also underlie behavioral observations (Luján and Aguado, 2015; Golan et al., 2016).

Together, our data suggest that since GIRK channels regulate neural excitability, they appear to be essential for normal hippocampal performance at synaptic level, playing a pivotal role in LTP/LTD threshold regulation and in the induction and maintenance of plasticity processes.

GIRK channel activity is essential for non-associative and associative hippocampal-dependent memory

When non-associative habituation learning was tested in the OF task, we found i.c.v. GIRK modulation to produce retrieval, and probably more phases, deficits of exploratory habituation memory consistent with excitability and LTP impairments observed both *ex vivo* and *in vivo*. It has recently been shown that hippocampal hyperexcitability and plasticity deficits induced by acute amyloidopathy also impaired exploratory habituation in mice (Mayordomo-Cava et al., 2020; Sánchez-Rodríguez et al., 2020). Interestingly, i.c.v. metaplastic GIRK activation reestablished LTP and hippocampal-dependent memory retrieval (Sánchez-Rodríguez et al., 2017, 2020), as also proposed in other amyloidosis models (Li et al., 2017; Peineau et al., 2018). Moreover, intraperitoneal administration of VU0466551, a twofold improved-potency ML297 analog, increased exploratory activity (Abney et al., 2019) while reducing GIRK-dependent signaling either constitutively (Pravetoni and Wickman, 2008) or selectively in dorsal hippocampus (Victoria et al., 2016), produced hyperactivity. Nevertheless, ML297/TQ i.c.v. injections did not alter motor function, stress, or anxiety levels. Therefore, our results suggest the importance of hippocampal GIRK conductance to sustain plasticity processes involved in exploratory habituation memory retrieval.

GIRK activity modulation by i.c.v. injections also impaired recognition memory retrieval. Recognition memory and

hippocampal synaptic plasticity processes are also regulated through an inhibitory control mediated by 5-HT1A receptors (Fernández et al., 2017), as their selective pharmacological activation has been shown to facilitate synaptic strength depotentiation (Fernández et al., 2017), very likely through GIRK channels in a similar mechanism to that reported here. Furthermore, basal GIRK conductance has been associated to adenosine A_1R constitutive activity in the hippocampus (Kim and Johnston, 2015). A_1R activation induces an LTP depotentiation to prepare hippocampal synapses for subsequent synaptic processing and avoid synaptic overload (Izumi and Zorumski, 2019). We demonstrated *in vivo* that such mechanism requires GIRK channels to operate (Sánchez-Rodríguez et al., 2019) in a way compatible with A_1R-GIRK association found in the present work. In fact, the inhibition of A_1R has been shown to block depotentiation in CA1 hippocampal region, suggesting a role in memory erasure (Madroñal et al., 2016). However, present data do not preclude the possible impact on plasticity processes of G-protein-independent GIRK activity or GIRK channel activity regulated by other GPCRs different to A_1Rs.

Finally, we showed that modulation of hippocampal GIRK activity also impacts on associative LTM, as it was needed for acquiring a complex operant task. The hippocampus is one of the regions involved in both acquisition and storage of associative learning, such as operant conditioning (Gruart et al., 2015; Jurado-Parras et al., 2016). In fact, the lack of presynaptic $GABA_B$ receptors (of which GIRK channels are main effectors) at hippocampal glutamatergic synapses also impaired acquisition of an operant learning task (Jurado-Parras et al., 2016), suggesting the critical GIRK channels contribution to certain forms of associative learning (Pravetoni and Wickman, 2008).

In summary, we found that GIRK channel activity adjusts the dorsal hippocampus synapses to undertake the activity required for memory formation or retrieval. When this metaplastic mechanism fails, marked deleterious changes are produced in hippocampal cognitive functions such as learning an associative instrumental task or recalling familiar objects and environments. Consequently, GIRK channels gain relevance as main determinants of neuronal excitability to support hippocampal-dependent cognitive functions.

References

Abney KK, Bubser M, Du Y, Kozek KA, Bridges TM, Linsdley CW, Daniels JS, Morrison RD, Wickman K, Hopkins CR, Jones CK, Weaver CD (2019) Analgesic effects of the GIRK activator, VU0466551, alone and in combination with morphine in acute and persistent pain models. ACS Chem Neurosci 10:1294–1299.

Abraham WC (2008) Metaplasticity: tuning synapses and networks for plasticity. Nat Rev Neurosci 9:387.

Bliss TV, Gardner-Medwin AR (1973) Long-lasting potentiation of synaptic transmission in the dentate area of the unanaestetized rabbit following stimulation of the perforant path. J Physiol 232:357–374.

Bliss TV, Collingridge GL, Laroche S (2006) Neuroscience. ZAP and ZIP, a story to forget. Science 313:1058–1059.

Bliss TV, Collingridge GL, Morris R (2007) Synaptic plasticity in the hippocampus. In: The hippocampus book (Andersen P, Morris R, Amaral DG, Bliss T, ÓKeefe J, eds), pp 343–474. New York: Oxford University Press.

Bliss T, Collingridge GL, Morris R, Reymann KG (2018) Long-term potentiation in the hippocampus: discovery, mechanisms and function. Neuroforum 24:A103–A120.

Buttner D (1991) Climbing on the cage lid, a regular component of locomotor activity in the mouse. J Exp Anim Sci 34:165–169.

Chen X, Johnston D (2005) Constitutively active G-protein-gated inwardly rectifying K+ channels in dendrites of hippocampal CA1 pyramidal neurons. J Neurosci 25:3787–3792.

Chung HJ, Ge WP, Qian X, Wiser O, Jan YN, Jan LY (2009) G protein-activated inwardly rectifying potassium channels mediate depotentiation of long-term potentiation. Proc Natl Acad Sci USA 106:635–640.

Clarke JR, Cammarota M, Gruart A, Izquierdo I, Delgado-García JM (2010) Plastic modifications induced by object recognition memory processing. Proc Natl Acad Sci USA 107:2652–2657.

Collingridge GL, Peineau S, Howland JG, Wang YT (2010) Long-term depression in the CNS. Nat Rev Neurosci 11:459–473.

Cooper LN, Bear MF (2012) The BCM theory of synapse modification at 30: interaction of theory with experiment. Nat Rev Neurosci 13:798–810.

Cummings JA, Mulkey RM, Nicoll RA, Malenka RC (1996) Ca2+ signaling requirements for long-term depression in the hippocampus. Neuron 16:825–833.

Davies CH, Starkey SJ, Pozza MF, Collingridge GL (1991) GABA autoreceptors regulate the induction of LTP. Nature 349:609–611.

Days E, Kaufmann K, Romaine I, Niswender C, Lewis M, Utley T, Du Y, Sliwoski G, Morrison R, Dawson ES, Engers JL, Denton J, Daniels JS, Sulikowski GA, Lindsley CW, Weaver CD (2010) Discovery and Characterization of a Selective Activator of the G-Protein Activated Inward-Rectifying Potassium (GIRK) Channel. In: Probe Reports from the NIH Molecular Libraries Program [Internet]. Bethesda, MD: National Center for Biotechnology Information (US).

Dembitskaya Y, Wu YW, Semyanov A (2020) Tonic GABAA conductance favors spike-timing-dependent over theta-burst-induced long-term potentiation in the hippocampus. J Neurosci 40:4266–4276.

DeVos SL, Miller TM (2013) Direct intraventricular delivery of drugs to the rodent central nervous system. J Vis Exp. Advance online publication. Retrived May 12, 2013. doi: 10.3791/50326.

Drake CT, Bausch SB, Milner TA, Chavkin C (1997) GIRK1 immunoreactivity is present predominantly in dendrites, dendritic spines, and somata in the CA1 region of the hippocampus. Proc Natl Acad Sci USA 94:1007–1012.

Etkin A, Alarcón JM, Weisberg SP, Touzani K, Huang YY, Nordheim A, Kandel ER (2006) A role in learning for SRF: deletion in the adult forebrain disrupts LTD and the formation of an immediate memory of a novel context. Neuron 50:127–143.

Fanselow MS, Dong HW (2010) Are the dorsal and ventral hippocampus functionally distinct structures? Neuron 65:7–19.

Fernández-Alacid L, Watanabe M, Molnár E, Wickman K, Luján R (2011) Developmental regulation of G protein-gated inwardly-rectifying K+ (GIRK/Kir3) channel subunits in the brain. Eur J Neurosci 34:1724–1736.

Fernández-Lamo I, Delgado-García JM, Gruart A (2018) When and where learning is taking place: multisynaptic changes in strength during different behaviors related to the acquisition of an operant conditioning task by behaving rats. Cereb Cortex 28:1011–1023.

Fernández SP, Muzerelle A, Scotto-Lomassese S, Barik J, Gruart A, Delgado-García JM, Gaspar P (2017) Constitutive and acquired serotonin deficiency alters memory and hippocampal synaptic plasticity. Neuropsychopharmacology 42:512–523.

Golan DA, Armstrong EJ, Armstrong AW (2016) Principles of pharmacology: the pathophysiologic basis of drug therapy, Ed 4. Philadelphia: Lippincott Williams and Wilkins.

González C, Baez-Nieto D, Valencia I, Oyarzún I, Rojas P, Naranjo D, Latorre R (2012) K(+) channels: function-structural overview. Compr Physiol 2:2087–2149.

Gruart A, Delgado-García JM (2007) Activity-dependent changes of the hippocampal CA3-CA1 synapse during the acquisition of associative learning in conscious mice. Genes Brain Behav 6 [Suppl 1]:24–31.

Gruart A, Muñoz MD, Delgado-García JM (2006) Involvement of the CA3-CA1 synapse in the acquisition of associative learning in behaving mice. J Neurosci 26:1077–1087.

Gruart A, Benito E, Delgado-García JM, Barco A (2012) Enhanced cAMP response element-binding protein activity increases neuronal excitability, hippocampal long-term potentiation, and classical eyeblink conditioning in alert behaving mice. J Neurosci 32:17431–17441.

Gruart A, Leal-Campanario R, López-Ramos JC, Delgado-García JM (2015) Functional basis of associative learning and its relationships with long-term potentiation evoked in the involved neural circuits: lessons from studies in behaving mammals. Neurobiol Learn Mem 124:3–18.

Hardt O, Nader K, Wang YT (2014) GluA2-dependent AMPA receptor endocytosis and the decay of early and late long-term potentiation: possible mechanisms for forgetting of short- and long-term memories. Philos Trans R Soc Lond B Biol Sci 369:20130141.

Hasan MT, Hernández-González S, Dogbevia G, Treviño M, Bertocchi I, Gruart A, Delgado-García JM (2013) Role of motor cortex NMDA receptors in learning-dependent synaptic plasticity of behaving mice. Nat Commun 4:2258.

Hill E, Hickman C, Diez R, Wall M (2020) Role of A1 receptor-activated GIRK channels in the suppression of hippocampal seizure activity. Neuropharmacology 164:107904.

Huang CS, Shi SH, Ule J, Ruggiu M, Barker LA, Darnell RB, Jan YN, Jan LY (2005) Common molecular pathways mediate long-term potentiation of synaptic excitation and slow synaptic inhibition. Cell 123:105–118.

Izumi Y, Zorumski CF (2019) Temperoammonic stimulation depotentiates Schaffer collateral LTP via p38 MAPK downstream of adenosine A1 receptors. J Neurosci 39:1783–1792.

Jeremic D, Sánchez-Rodríguez I, Jimenez-Diaz L, Navarro-Lopez JD (2021) Therapeutic potential of targeting G protein-gated inwardly rectifying potassium (GIRK) channels in the central nervous system. Pharmacol Ther 223:107808.

Jin W, Lu Z (1998) A novel high-affinity inhibitor for inward-rectifier K+ channels. Biochemistry 37:13291–13299.

Jurado-Parras MT, Delgado-García JM, Sánchez-Campusano R, Gassmann M, Bettler B, Gruart A (2016) Presynaptic GABAB receptors regulate hippocampal synapses during associative learning in behaving mice. PLoS One 11:e0148800.

Kalueff AV, Tuohimaa P (2004) Grooming analysis algorithm for neurobehavioural stress research. Brain Res Brain Res Protoc 13:151–158.

Keck T, Hübener M, Bonhoeffer T (2017) Interactions between synaptic homeostatic mechanisms: an attempt to reconcile BCM theory, synaptic scaling, and changing excitation/inhibition balance. Curr Opin Neurobiol 43:87–93.

Kim CS, Johnston D (2015) A1 adenosine receptor-mediated GIRK channels contribute to the resting conductance of CA1 neurons in the dorsal hippocampus. J Neurophysiol 113:2511–2523.

Koyrakh L, Luján R, Colón J, Karschin C, Kurachi Y, Karschin A, Wickman K (2005) Molecular and cellular diversity of neuronal G-protein-gated potassium channels. J Neurosci 25:11468–11478.

La-Vu M, Tobias BC, Schuette PJ, Adhikari A (2020) To approach or avoid: an introductory overview of the study of anxiety using rodent assays. Front Behav Neurosci 14:145.

Leussis MP, Bolivar VJ (2006) Habituation in rodents: a review of behavior, neurobiology, and genetics. Neurosci Biobehav Rev 30:1045–1064.

Li Q, Navakkode S, Rothkegel M, Soong TW, Sajikumar S, Korte M (2017) Metaplasticity mechanisms restore plasticity and associativity in an animal model of Alzheimer's disease. Proc Natl Acad Sci USA 114:5527–5532.

Lopes BC, Medeiros LF, Stein DJ, Cioato SG, de Souza VS, Medeiros HR, Sanches PRS, Fregni F, Caumo W, Torres ILS (2021) tDCS and exercise improve anxiety-like behavior and locomotion in chronic pain rats via modulation of neurotrophins and inflammatory mediators. Behav Brain Res 404:113173.

Luján R, Aguado C (2015) Localization and targeting of GIRK channels in mammalian central neurons. Int Rev Neurobiol 123:161–200.

Luján R, Marron Fernández de Velasco E, Aguado C, Wickman K (2014) New insights into the therapeutic potential of Girk channels. Trends Neurosci 37:20–29.

Lüscher C, Slesinger PA (2010) Emerging roles for G protein-gated inwardly rectifying potassium (GIRK) channels in health and disease. Nat Rev Neurosci 11:301–315.

Lüscher C, Malenka RC (2012) NMDA receptor-dependent long-term potentiation and long-term depression (LTP/LTD). Cold Spring Harb Perspect Biol 4:a005710.

Lüscher C, Jan LY, Stoffel M, Malenka RC, Nicoll RA (1997) G protein-coupled inwardly rectifying K+ channels (GIRKs) mediate postsynaptic but not presynaptic transmitter actions in hippocampal neurons. Neuron 19:687–695.

Madroñal N, Delgado-García JM, Gruart A (2007) Differential effects of long-term potentiation evoked at the CA3 CA1 synapse before, during, and after the acquisition of classical eyeblink conditioning in behaving mice. J Neurosci 27:12139–12146.

Madroñal N, Delgado-García JM, Fernández-Guizan A, Chatterjee J, Kohn M, Mattucci C, Jain A, Tsetsenis T, Illarionova A, Grinevich V, Gross CT, Gruart A (2016) Rapid erasure of hippocampal memory following inhibition of dentate gyrus granule cells. Nat Commun 7:10923.

Malik R, Johnston D (2017) Dendritic GIRK channels gate the integration window, plateau potentials, and induction of synaptic plasticity in dorsal but not ventral CA1 neurons. J Neurosci 37:3940–3955.

Malleret G, Alarcon JM, Martel G, Takizawa S, Vronskaya S, Yin D, Chen IZ, Kandel ER, Shumyatsky GP (2010) Bidirectional regulation of hippocampal long-term synaptic plasticity and its influence on opposing forms of memory. J Neurosci 30:3813–3825.

Mayfield J, Blednov YA, Harris RA (2015) Behavioral and genetic evidence for GIRK channels in the CNS: role in physiology, pathophysiology, and drug addiction. Int Rev Neurobiol 123:279–313.

Mayordomo-Cava J, Iborra-Lázaro G, Djebari S, Temprano-Carazo S, Sánchez-Rodríguez I, Jeremic D, Gruart A, Delgado-García JM, Jiménez-Díaz L, Navarro-López JD (2020) Impairments of synaptic plasticity induction threshold and network oscillatory activity in the hippocampus underlie memory deficits in a non-transgenic mouse model of amyloidosis. Biology 9:175.

Morris R (2007) Theories of hippocampal function. In: The hippocampus book (Andersen P, Morris R, Amaral DG, Bliss T, O' Keefe J, eds), pp 581–713. New York: Oxford University Press.

Nava-Mesa MO, Jiménez-Díaz L, Yajeya J, Navarro-Lopez JD (2013) Amyloid-beta induces synaptic dysfunction through G protein-gated inwardly rectifying potassium channels in the fimbria-CA3 hippocampal synapse. Front Cell Neurosci 7:117.

Nava-Mesa MO, Jimenez-Diaz L, Yajeya J, Navarro-Lopez JD (2014) GABAergic neurotransmission and new strategies of neuromodulation to compensate synaptic dysfunction in early stages of Alzheimer's disease. Front Cell Neurosci 8:167.

Ostrovskaya O, Xie K, Masuho I, Fajardo-Serrano A, Luján R, Wickman K, Martemyanov KA (2014) RGS7/Gβ5/R7BP complex regulates synaptic plasticity and memory by modulating hippocampal GABABR-GIRK signaling. Elife 3:e02053.

Paxinos G, Franklin KB (2001) The mouse brain in stereotaxic coordinates. London: Academic Press.

Peineau S, Rabiant K, Pierrefiche O, Potier B (2018) Synaptic plasticity modulation by circulating peptides and metaplasticity: involvement in Alzheimer's disease. Pharmacol Res 130:385–401.

Platel A, Porsolt RD (1982) Habituation of exploratory activity in mice: a screening test for memory enhancing drugs. Psychopharmacology (Berl) 78:346–352.

Pravetoni M, Wickman K (2008) Behavioral characterization of mice lacking GIRK/Kir3 channel subunits. Genes Brain Behav 7:523–531.

Reis SL, Silva HB, Almeida M, Cunha RA, Simoes AP, Canas PM (2019) Adenosine A1 and A2A receptors differently control synaptic plasticity in the mouse dorsal and ventral hippocampus. J Neurochem 151:227–237.

Rifkin RA, Moss SJ, Slesinger PA (2017) G protein-gated potassium channels: a link to drug addiction. Trends Pharmacol Sci 38:378–392.

Rishal I, Porozov Y, Yakubovich D, Varon D, Dascal N (2005) Gβγ-dependent and Gβγ-independent basal activity of G protein-activated K+ channels. J Biol Chem 280:16685–16694.

Sánchez-Rodríguez I, Temprano-Carazo S, Nájera A, Djebari S, Yajeya J, Gruart A, Delgado-García JM, Jiménez-Díaz L, Navarro-López JD (2017) Activation of G-protein-gated inwardly rectifying potassium (Kir3/GirK) channels rescues hippocampal functions in a mouse model of early amyloid-beta pathology. Sci Rep 7:14658.

Sánchez-Rodríguez I, Gruart A, Delgado-García JM, Jimenez-Diaz L, Navarro-Lopez JD (2019) Role of GirK channels in long-term potentiation of synaptic inhibition in an in vivo mouse model of early amyloid-β pathology. Int J Mol Sci 20:1168.

Sánchez-Rodríguez I, Djebari S, Temprano-Carazo S, Vega-Avelaira D, Jiménez-Herrera R, Iborra-Lázaro G, Yajeya J, Jiménez-Díaz L, Navarro-López JD (2020) Hippocampal long-term synaptic depression and memory deficits induced in early amyloidopathy are

prevented by enhancing G-protein-gated inwardly rectifying potassium channel activity. J Neurochem 153:362–376.
Slesinger PA, Wickman K (2015) Structure to function of G protein-gated inwardly rectifying (GIRK) channels, Ed 1. San Diego: Elsevier Inc.
Trompoukis G, Rigas P, Leontiadis LJ, Papatheodoropoulos C (2020) Ih, GIRK, and KCNQ/Kv7 channels differently modulate sharp wave - ripples in the dorsal and ventral hippocampus. Mol Cell Neurosci 107:103531.
Victoria NC, Marron Fernández de Velasco E, Ostrovskaya O, Metzger S, Xia Z, Kotecki L, Benneyworth MA, Zink AN, Martemyanov KA, Wickman K (2016) G protein-gated K+ ghannel ablation in forebrain pyramidal neurons selectively impairs fear learning. Biol Psychiatry 80:796–806.
Villarreal DM, Do V, Haddad E, Derrick BE (2002) NMDA receptor antagonists sustain LTP and spatial memory: active processes mediate LTP decay. Nat Neurosci 5:48–52.
Walf AA, Frye CA (2007) The use of the elevated plus maze as an assay of anxiety-related behavior in rodents. Nat Protoc 2:322–328.
Wetherington JP, Lambert NA (2002) Differential desensitization of responses mediated by presynaptic and postsynaptic A1 adenosine receptors. J Neurosci 22:1248–1255.
Xiong G, Metheny H, Johnson BN, Cohen AS (2017) A comparison of different slicing planes in preservation of major hippocampal pathway fibers in the mouse. Front Neuroanat 11:107.
Zucker RS, Regehr WG (2002) Short-term synaptic plasticity. Annu Rev Physiol 64:355–405.